Science of the Total Environment 771 (2021) 145186

Contents lists available at ScienceDirect

Science of the Total Environment

journal homepage: www.elsevier.com/locate/scitotenv

Doubling of the population exposed to drought over South Asia: CMIP6 multi-model-based analysis

Sanjit Kumar Mondal [a,1], Jinlong Huang [a,1], Yanjun Wang [a], Buda Su [a,c,*], Jianqing Zhai [a,b], Hui Tao [c], Guojie Wang [a], Thomas Fischer [d], Shanshan Wen [a], Tong Jiang [a,c,*]

[a] Collaborative Innovation Center on Forecast and Evaluation of Meteorological Disasters/Institute for Disaster Risk Management/School of Geographical Science, Nanjing University of Information Science & Technology, Nanjing 210044, China
[b] National Climate Center, China Meteorological Administrations, Beijing 100081, China
[c] State Key Laboratory of Desert and Oasis Ecology, Xinjiang Institute of Ecology and Geography, Chinese Academy of Sciences, Urumqi 830011, China
[d] Department of Geosciences, Eberhard Karls University, Tübingen 72070, Germany

HIGHLIGHTS

- The highest increase in South Asian population exposure to drought (2.3-fold) is projected under the SSP3-7.0 scenario.
- Population exposure is >1.5-fold higher in the near-term and mid-term periods under selected SSP-RCP scenarios.
- In the near-term period, climate change effect is the key contributor in exposure changes in South Asia.

GRAPHICAL ABSTRACT

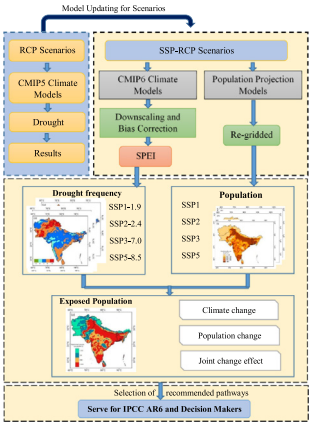

ARTICLE INFO

Article history:
Received 12 November 2020
Received in revised form 10 January 2021
Accepted 10 January 2021
Available online 6 February 2021

Editor: Fernando A.L. Pacheco

Keywords:
Climate change
Exposure
Drought
CMIP6

ABSTRACT

Drought has a substantial socioeconomic impact under the changing climate. The estimation of population exposure to drought could be the pivotal signal to predict future water scarcity in the climate hotspot of South Asia. This study examines the changing population exposure to drought across South Asia using 20 climate model ensembles from the latest CMIP6 and demographic data under shared socioeconomic pathways (SSPs). Underpinning the latest version of the IPCC 6th Assessment Report (AR6), this paper focuses on the 2021–2040 (near-term), 2041–2060 (mid-term), and 2081–2100 (long-term) periods to project population exposure changes relative to the reference period (1995–2014) under four SSP-RCP scenarios. Drought events are detected by adopting the standardized precipitation evapotranspiration index (SPEI) and run theory method. Model validation suggests that CMIP6-GCM performs well in projecting climate variables and capturing drought events. The results show that the projected increases in frequent drought events and affected areal coverage are stronger during the early part of the century and weaker at the end under all scenario combinations. In relative terms, the projected increase in the number of people exposed to drought is dominant (>1.5-fold) in the near-

* Corresponding authors at: Collaborative Innovation Center on Forecast and Evaluation of Meteorological Disasters/Institute for Disaster Risk Management/School of Geographical Science, Nanjing University of Information Science & Technology, Nanjing 210044, China.
E-mail addresses: subd@cma.gov.cn (B. Su), jiangtong@nuist.edu.cn (T. Jiang).
[1] First authors (equal contribution): Sanjit Kumar Mondal and Jinlong Huang.

https://doi.org/10.1016/j.scitotenv.2021.145186

SSPs-RCPs scenario
SPEI
South Asia

term and mid-term periods but decreases in the long-term period. Compared to the reference period, the leading increase in population exposure (2.3-fold) is projected under the newly designed gap scenario (SSP3–7.0) in the mid-term period. A surprising decline in the number of exposed populations was estimated to be 18.8% under SSP5–8.5 by the end of the century. The mitigating effect of the predicted heavy precipitation will decrease droughts in the late future. Spatially, increasing exposure will become more pronounced across India and Afghanistan. Furthermore, the population change effect is mainly responsible for the exposure changes in South Asia. However, this study strongly recommends future 'plausible world' regional rivalry pathways (SSP3) scenario-combinations into consideration for policymaking in regard to water management as well as migration planning over South Asia.

1. Introduction

Climate-change-related risks are mostly investigated by functions of hazards, vulnerability and exposure of the population, economy, society, and natural environment (IPCC, 2013). In general, humans ultimately suffer from all hazards. The vulnerability of a population to a particular hazard can vary due to age, season and geographic region (Barnett et al., 2010). Human vulnerability can be measured by evaluating exposure, sensitivity of society to hazards, and capacity to combat (UNISDR, 2009; Field et al., 2012). With changing warming levels, the climate risks to human safety, health, livelihood, and water availability are predicted to increase. Adaptation to climate change and associated risk management emphasis on reducing exposure and vulnerability (IPCC, 2012).Therefore, the estimation of exposure is recognized as a fundamental aspect of any disaster loss and risk assessment.

Drought is the most recurring and complicated weather-driven natural hazard globally (UNISDR, 2009; WMO, 2013). Droughts across different climate zones are likely to become worse in terms of the more frequent occurrence of severe drought events. Rising water demands due to extensive human activities and alterations to hydro-climatological environments with critical warming levels will trigger drought impacts. Drought has substantial effects on society, the economy, and ecosystems in all climate belts (Trenberth et al., 2015; Su et al., 2018). Droughts rank first among all the devastating natural disasters regarding the exposed population (Mishra and Singh, 2010). An increased portion of the population is anticipated to be exposed to water scarcity due to the rising population and varying climate (Watts et al., 2015). The International Disaster Database (hattps://www.emdat.be/) recorded that there were 2.71×10^9 drought-affected persons globally and 11,731,294 deaths, and the estimated economic losses were 1.745×10^{11} US$ during the historical time frame of 1900–2019. Unfortunately, global drying features and the associated damage are anticipated to increase in the future under a changing climate. Drought frequency, intensity, and duration are likely to escalate in a warming world with an increase in atmospheric greenhouse gas concentrations (IPCC, 2013; Chen and Sun, 2015; Donohue et al., 2010; van der Schrier et al., 2011) stated that. In the socioeconomic structure, the population is highly sensitive to drought, as it directly impacts the water and food supply (Wilhite et al., 2014). Therefore, it is of great concern to policymakers how future socioeconomic exposure to drought would unfold with different warming trajectories, especially at the regional and local scales. Therefore, it is urgent to determine how droughts could be provoked, propagate, and affect us in terms of rate, degree, and location to enhance drought adaptation and mitigation plans.

South Asia is characterized as a climate-sensitive region. South Asian countries are recognized to have large populations, where India, Pakistan, and Bangladesh have been highlighted among the countries that are extremely vulnerable to a changing climate globally (Global Climate Risk Index, 2018). The World Bank (2016) reported that approximately 67% of people across South Asia live in rural areas and maintain their livelihoods by depending on agriculture. Population growth and extending economic growth will increase the water demands in this region. Over the region, an acute water shortage will cause GDP losses of 6% by the middle of the century (World Bank, 2016). South Asian countries are extremely vulnerable to different severe climate-change-related events, such as drought, floods, and heatwaves (Su et al., 2016; Huang et al., 2017). It is expected that heat waves will further lead to drought, resulting in local food production and crop failure (Schleussner et al., 2018). Due to severe drought, the Pakistani agricultural sector recorded 2.6% negative growth in 2002 and reported that ~3.3 million people were exposed drought (Ahmad et al., 2004). During droughts in 2002 and 2014, a large number of people (>300 million) in India were exposed (Barthel and Neumayer, 2012; Mishra et al., 2016). The occurrence of a severe drought event in the southern part of India led to impacts to >0.2 million people in 2017 (Aadhar and Mishra, 2017). Therefore, anticipating the changes in population exposure to drought under different climate change scenarios is pivotal to unfolding future vulnerability in terms of formulating mitigation plans for policymakers.

Drought indices and hydro-meteorological variables are intuitive for characterizing drought events. In terms of the relative effectiveness of different indices, the multi-scalar standardized precipitation evapotranspiration index (SPEI) developed by Vicente-Serrano et al. (2010) is widely accepted to quantify extreme dry and wet events under a warming-induced changing climate. The sensitivity of the SPEI to precipitation and potential evapotranspiration (PET) demonstrates clear geographic variation across different climate regions. In general, intense dryness is detected by the SPEI in tropical and subtropical regions. In semiarid regions, the SPEI reflects strong dryness in response to PET, while it shows sensitivity to precipitation (wetness) in humid regions (Vicente-Serrano et al., 2015). In Ningxia, China (an arid and semiarid region), the SPEI yields a long average drought duration, high intensity and frequent drought events due to the low precipitation and high evaporation in the area (Tan et al., 2015). Furthermore, Irannezhad et al. (2017) reported that the SPEI is practically effective in deterring drought across cold regions, where drought during the winter is influenced by precipitation variations but drought during the warm season is influenced by increased PET.

It is apparent that the global climate model (GCM) outputs from the Coupled Model Intercomparison Project (CMIP) have been imperative in assessing future climatic risks (i.e., drought). In this study, we quantified the anticipated changes in the population exposed to drought using GCM projections from the new sixth phase of the CMIP (CMIP6) (Eyring et al., 2016) and demographic changes under five new shared socioeconomic pathways (SSPs). There are almost 30 improved GCM outputs available in CMIP6 that were incorporated by various modelling centres. Different emission scenarios with different forcing trajectories are designed under the Scenario Model Intercomparison Project (ScenarioMIP) as the core of the 6th phase. In this latest phase, scenario combinations are derived from shared socioeconomic pathways (SSPs) and representative concentration pathways (RCPs). The new scenario layout that links the RCPs with SSPs (SSPs-RCPs) is derived based on integrating the future pathway of exposure and vulnerability concepts under a changing climate. Considering the effects of climate change and policies, five new shared socioeconomic pathways (SSPs) have

been designed to unfold probable evolutions of future socio-demographic advancement in the 21st century. The SSPs denote sustainability (SSP1), middle of the road with the historical trend (SSP2), fragmentation (SSP3), inequality (SSP4), and the growth-oriented world (SSP5) (O'Neill et al., 2017). In this study, we use 20 GCM outputs for four SSP-RCP scenarios from CMIP6 and future demographic changes under five SSPs to demarcate an inclusive depiction to realize forthcoming changes in population exposure to drought over South Asia.

Overwhelming societal impacts of intense drought have drawn the utmost attention worldwide. Numerous studies have emphasized the evolution of prospective changes in drought frequency and magnitude, whereas negligible effort has been paid to exploring vulnerability changes. This study aims to analyse the changes in the population exposed to drought in the future, as well as to elucidate the significance of a changing climate and growing population in exposure changes. This research focus on analytically measuring the affected population under anticipated drought conditions across South Asia considering the influential effects of climate change and population change. In specific terms, using the upgraded GCM outputs from CMIP6, this study intends to elucidate the following three questions: (i) To what degree can the population be exposed to drought under different SSP-RCP scenarios? (ii) At which time horizon exposure could the peak be reached by the 21st century? (iii) How do the three targeted causal factors (population change effect, climate change effect, and population-climate interaction effect) influence exposure changes? However, as far as the authors know, this is the first attempt using the latest CMIP6 model outputs to study future population exposure to drought in South Asia that considers the entire region. Furthermore, it is believed that the advancement in up-to-date GCMs could provide more realistic and consistent results across South Asian countries, which can be taken as the fundamental basis to induce policy interventions for drought risk mitigation and adaptation.

2. Datasets and methods

2.1. Study area

This study was conducted in the South Asia region, which is located at 5°N to 40°N and 60°E to 100°E (Fig. 1). The region encompasses a large land area of approximately 5.2 million km^2. India is recognized as the largest country in terms of both population and area coverage among the seven continental countries (Afghanistan, Bangladesh, Bhutan, India, Nepal, Pakistan, and Sri Lanka) of the South Asian domain. Furthermore, the dynamic climatology of this region is mostly determined by complex monsoon systems. Meteorologically, South Asian countries feature long periods of maximum temperatures, humidity, and varying precipitation. Based on the Köppen—Geiger climate classification system, the domain can be characterized as the arid zone in the west, tropical zone in the east, and temperate zone in the northern part. In terms of altitude, the northern part is dominated by high elevations that decrease towards the southern part. The geographical location and elevation above mean sea level are represented in Fig. 1.

2.2. Datasets

The state-of-the-art CMIP6 framework has evolved to meet the demand of a growing scientific community by improving the drawbacks in CMIP5 (Eyring et al., 2016). Recently, CMIP6-GCMs have become pivotal features in driving climate research across the globe. In this study, historical and future simulations from the latest CMIP6 archive are applied to anticipate future drought in South Asia. In this aspect, this study analysed the following monthly climatological parameters: precipitation, maximum temperature, minimum temperature, wind speed, shortwave solar radiation, and surface relative humidity, as well as surface soil moisture and surface runoff for the periods of

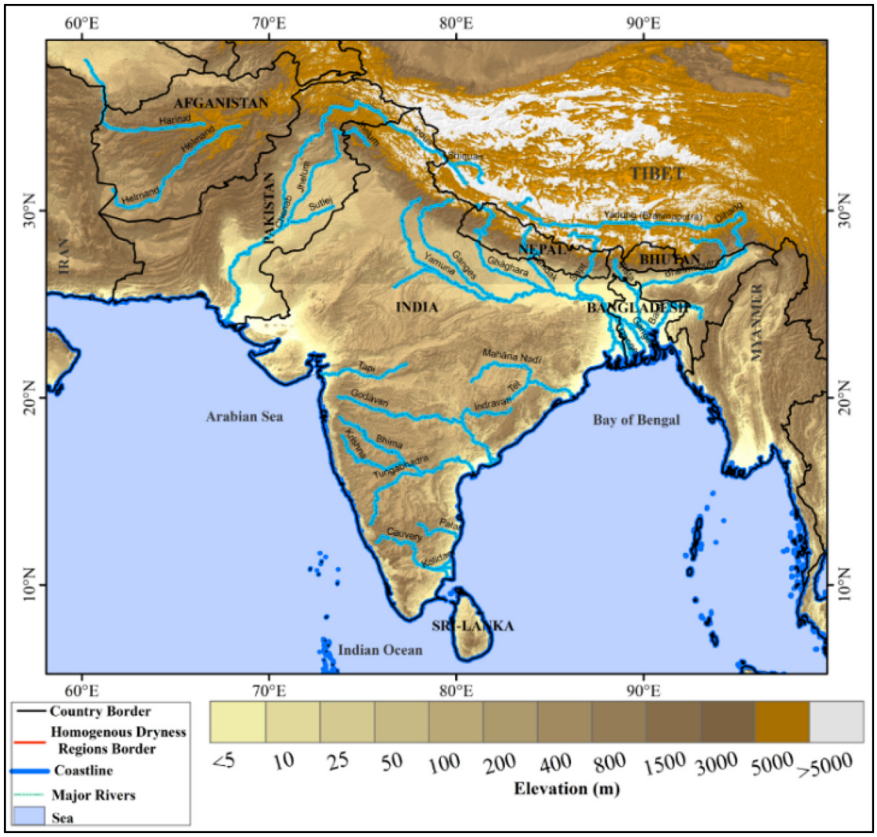

Fig. 1. Elevation map of South Asia.

1995–2014 and 2021–2100. Considering the availability of all the aforementioned required variables, this research work selected 20 GCMs from CMIP6, as presented in Table 1. In the time of writing this paper, only 20 GCMs made all the required parameters available under four common SSP-RCP scenarios, namely, SSP1–2.6, SSP2–4.5, SSP3–7.0, and SSP5–8.5. These four scenarios (maximum) were common among all 20 selected GCMs that contained all the required variables. The selected SSP-RCPs are regarded as combinations of low societal vulnerability with a low emission level (SSP1–2.6), intermediate societal vulnerability with an intermediate emission range (SSP2–4.5), comparatively high societal vulnerability with a medium to high forcing range (SSP3–7.0), and SSP5–8.5 is considered higher emissions that impose high mitigation but low adaptation challenges (O'Neill et al., 2016). Furthermore, analysis in this study demonstrates that the selected GCMs still have uncertainties in simulating climate variables across South Asian countries. Therefore, to secure high resolution and reduce biases, we applied the widely recognized spatial disaggregation (SD) technique to downscale all the variables to a common horizontal grid at 0.5° × 0.5° resolution. Moreover, to proceed with further analysis with reduced biases, the Equidistant Cumulative Distribution Functions (EDCDF) method was used to perform bias correction against observed data. In this study, the detailed process of downscaling and bias correction was adopted by following Su et al. (2018).

Finally, to evaluate the representation of GCMs in capturing the South Asian climate, this work used reanalysis climate data for the period of 1995–2014. All the required parameters (monthly precipitation, maximum temperature, minimum temperature, wind speed, shortwave solar radiation, and surface relative humidity) were downloaded from the Inter-Sectoral Impact Model Intercomparison Project (ISIMIP) website. The ERA-Interim reanalysis data based on the WATCH Forcing Data methodology are known as the WFDEI. The ISIMIP makes these outputs available under the title of WFDEI and ERA-Interim data Merged and Bias-corrected for ISI-MIP (EWEMBI). These reanalysis climate parameters are further used to calculate potential evapotranspiration (PET). All the datasets are reprojected at 0.5° × 0.5° resolution.

The latest CMIP6 designed simulation period (historical) is 1850–2014 and projection period (future) 2015–2100. Tokarska et al. (2020) reported that the period 1995–2014 is supposed to be the base period in the IPCC sixth assessment report (AR6), since it's more consistent to AR5 base period in some extent. So, to expedite a better relative and statistical analysis for future periods considering IPCC forthcoming report, the historical simulation period 1995–2014 is selected as the 'reference period' in this paper. In addition, the periods of 2021–2040, 2041–2060, and 2081–2100 denote 'near-term', 'mid-term', and 'long-term' periods, respectively, which also underpin the IPCC AR6.

The country-level population data of South Asia for the 1995–2014 period were obtained from the World Bank. Future demographic changes under five SSPs for the period 2010–2100 were obtained from the ISI-MIP website. Among the five SSPs, SSP1, SSP2, and SSP3 accordingly signify low, intermediate, and high societal vulnerability, whereas SSP4 and SSP5 represent challenges in adaptation and mitigation (O'Neill et al., 2017). In this study, the spatial distribution of the population in 2015 over South Asia was downloaded from the GPWv4 website. The original resolution (30 arc *sec*) of the GPWv4 data was reprojected to 0.5° × 0.5° as a common resolution format. Notably, the population distribution under SSPs for the 2010–2100 period were deduced based on the gridded proportion of the population in 2015. The projection of the population distribution for 2010–2100 based on the spatial distribution of the 2015 population yields some uncertainties. Spatial bias may arise, which manifests an overestimation of the population in low-density areas and an underestimation of the spatial extent of the population in high-density areas. Projections may be presented in uninhibited areas such as pure cropland, forest, desert or pasture types. Key assumptions such as those regarding fertility, mortality, growth rate, urbanization level, internal or international migration and others could affect the population over some areas. Furthermore, this projection does

Table 1
Summary of the temporal and spatial resolution of the datasets used in the study.

Climate models from CMIP6

Model name	Institution with country	Temporal resolution	Spatial resolution (°)
ACCESS-CM2	Commonwealth Scientific and Industrial Research Organization- Australian Research Council Centre of Excellence for Climate System Science (CSRO-ARCCSS), Australia	1 month	1.2 × 1.8
ACCESS-ESM1–5	Commonwealth Scientific and Industrial Research Organization (ARCCSS), Australia		1.2 × 1.8
AWI-CM-1–1-MR	Alfred Wegener Institute, Helmholtz Centre for Polar and Marine Research, Germany'		0.9 × 0.9
CanESM5	Canadian Centre for Climate Modelling and Analysis, Environment and Climate Change, Canada		2.8 × 2.8
CanESM5-CanOE	Canadian Centre for Climate Modelling and Analysis, Environment and Climate Change, Canada		2.8 × 2.8
CESM2	National Center for Atmospheric Research (NCAR),USA		0.9 × 1.3
CMCC-CM2-SR5	Fondazione Centro Euro-Mediterraneo sui Cambiamenti Climatici, Italy		1.0 × 1.0
CNRM-CM6–1	Centre National de Recherches Meteorologiques- Centre Europeen de Recherche et de Formation Avancee en Calcul Scientifique (CNRM-CERFACS), France		1.4 × 1.4
CNRM-ESM2–1	Centre National de Recherches Meteorologiques- Centre Europeen de Recherche et de Formation Avancee en Calcul Scientifique (CNRM-CERFACS), France		1.4 × 1.4
FGOALS-g3	Chinese Academy of Sciences (CAS), China		2.3 × 2.0
GISS-E2–1-G	Goddard Institute for Space Studies (NASA-GISS), USA		2.0 × 2.5
INM-CM4–8	Institute for Numerical Mathematics, Russian Academy of Science, Russia		1.5 × 2.0
INM-CM5–0	Institute for Numerical Mathematics, Russian Academy of Science, Russia		1.5 × 2.0
IPSL-CM6A-LR	Institut Pierre Simon Laplace, France		1.3 × 2.5
MIROC6	Japan Agency for Marine-Earth Science and Technology, Japan		1.4 × 1.4
MIROC-ES2L	Japan Agency for Marine-Earth Science and Technology, Japan		2.7 × 2.8
MPI-ESM1–2-HR	Deutsches Klimarechenzentrum, Germany		~0.9
MPI-ESM1–2-LR	Max Planck Institute for Meteorology, Germany		~2.0
MRI-ESM2–0	Meteorological Research Institute, Japan		1.1 × 2.1
UKESM1–0-LL	Met Office Hadley Centre, UK		1.3 × 1.9

Population data

Data types	Organization/Institution	Temporal resolution	Spatial resolution (°)
Recorded population (temporal)	World bank	1 year	–
Gridded population of the World (GPWv4)	NASA's Earth Observing System Data and Information System		30 arc *sec*
Shared Socioeconomic Pathways (SSPs) based projection	Inter-Sectoral Impact Model Intercomparison Project		0.5 × 0.5

not consider the impact of climate change on the population distribution, as climate change influences population growth (Cao et al., 2012; Jiang et al., 2017; Wang et al., 2017; Jiang et al., 2018a, 2018b; Jiang et al., 2020b; Jing et al., 2020). Such uncertainties can be minimized using growth rates in future decades from the Revision of World Population Prospects (RWPP, United Nations, 2017a, b). This process provides a high-medium-low growth rate at each country level in each five-year increment. Furthermore, the revision of world urbanization prospects (RWUP, UN, 2018) used a sensitivity analysis using different growth rates from urban and rural areas to examine the possible movement between urban and rural areas. The consideration of different growth rates from RWPP and RWUP in population projections in China shows reduced uncertainties (Zhang et al., 2020). In addition, Jones and O'Neill (2016) used a parameterized gravity-based downscaling model to reduce the uncertainties in the United States population projection, which considers country-level or state-level growth rate, fertility, mortality, internal in-migration, internal out-migration, and international migration data from the US Census.

The temporal trend of the population recorded in 1995–2014 and projected in 2015–2100 and the spatial distribution of the population patterns in 2015 are shown in Fig. 2. The population in 2015 was approximately 1713 million in South Asia. Population changes are inclined to increase continuously under only the SSP3 scenario, whereas declines are observed for all other scenarios after a mid-century peak (Fig. 2a). Multi-year averaged population in 2021–2040 will be approximately 1750, 1843, 1947, 1817, and 1742 million under SSP1–5, respectively. In the period from 2041 to 2060, the population is projected to be 1869, 2109, 2429, 2033, and 1851 million, whereas the population will be 1564, 2108, 3180, 1942, and 1536 million in the long term (2081–2100). Projected population growth is higher in the mid-term period under all SSP scenarios than in the two other periods. The projected population in South Asia is subjective to be the greatest under the plausible world of fragmentation (SSP3), imposing high societal vulnerability. However, discerning the spatial structure of the population, the population distribution was comparatively low in the western part but high in the northern and southern parts of South Asia. The population density was >400 per km^2, mostly across the Indo-Gangetic Plain, including major populous cities, namely, Mumbai, Delhi, Bangalore, Hyderabad, and Ahmedabad of India; Karachi, Lahore, and Faisalabad of Pakistan; Colombo of Sri Lanka and all of Bangladesh.

2.3. Methods

2.3.1. Drought metric

It is suggested that PET-based drought indices such as the SPEI are preferable for measuring future droughts. Drought index performance evaluation-based studies have recommended that the SPEI is the best-suited index for assessing drought across South Asian countries (Gupta and Jain, 2018; Adnan et al., 2018). In this paper, drought is scrutinized by using the standardized precipitation evapotranspiration index (SPEI). The supply-demand function of the water balance theory is the core aspect of the SPEI. The 12-month scale for the SPEI is recognized as a vigorous representation of drought dynamics (Chen and Sun, 2015). The SPEI values increased with timescales, and droughts mostly responded to the SPEI with long timescales (Vicente-Serrano et al., 2012). Although SPEI-12 is mostly used to detect hydrological droughts, it also detects long-term meteorological drought. Long-term trends and inter-annual variations in droughts are well captured by the SPEI at the 12-month scale (Chen et al., 2018). The SPEI-12 month time scale is able to reflect both surface runoff and soil moisture deficit. Long-term droughts signify that both ground and surface water levels fall, resulting in substantial effects on socio-economic advancement. Here, we deduced the SPEI with a 12-month time scale in reflecting droughts across South Asia. The basic equation of the SPEI calculation is as follows:

$$D = P - PET \tag{1}$$

The water surplus or deficit over a climatic zone is reflected by the difference (D) between precipitation (P) and potential evapotranspiration (PET). The water balance of P-PET usually fits the log-logistic distribution. Since PET is the core input of the SPEI, the PET calculation process has an influential role in SPEI-based drought characterization. Biases in PET estimation trigger an overestimation of the drying trend (Sheffield et al., 2012). Among the different methods of PET calculation, the Food and Agriculture Organization (FAO) recommended that the Penman-Monteith method is a widely accepted method under changing climate conditions (Dai, 2011; Sheffield et al., 2012; Trenberth et al., 2014; Zhou et al., 2020). The Penman-Monteith equation followed by Allen et al. (1998) is as follows:

$$PET = \frac{0.408\Delta(R_n - G) + \gamma \frac{900}{T+273} U_2 (e_a - e_d)}{\Delta + \gamma(1 + 0.34u_2)} \tag{2}$$

where Δ is the slope of the saturation vapor pressure curve; T is the mean daily air temperature; e_a is the saturation vapor pressure; R_n is the net radiation at the surface; e_d is the actual atmospheric water vapor pressure; G is the all wave ground heat flux; γ is the psychometric constant; and u_2 is the daily average wind speed at 2 m height.

The reference period-driven log-logistic distribution coefficients are employed as the basis to estimate the drought index for the future period. The detailed SPEI calculation process is as Vicente-Serrano et al. (2010) suggested. In this work, dryness is diagnosed based on SPEI ≤−1. The lower the SPEI value is, the more severe the drought condition.

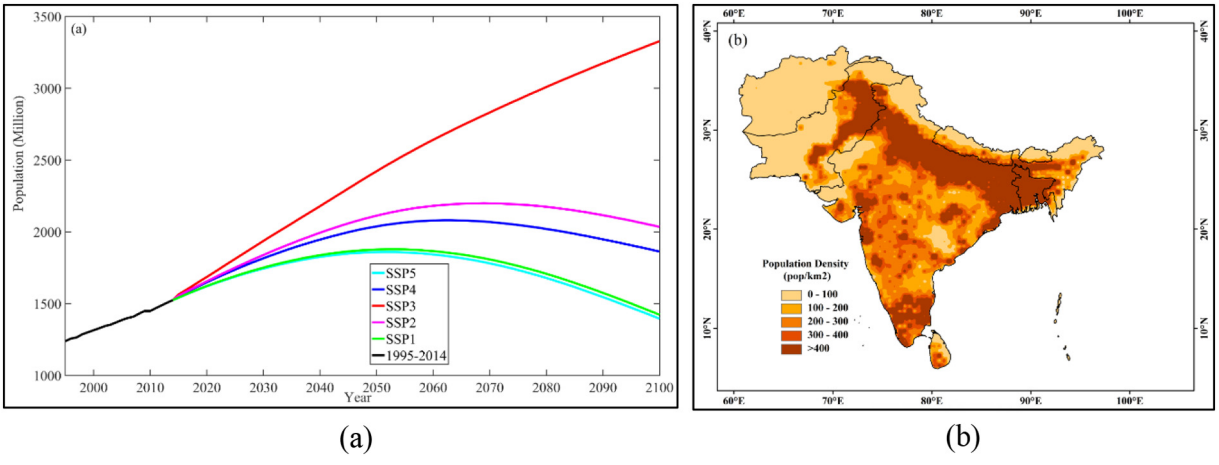

Fig. 2. (a) Recorded population for the 1995–2014 period and projected population for the 2015–2100 period. (b) Spatial pattern of the population density in South Asia in 2015.

Table S1 in the supplementary materials describes the different levels of different drought conditions.

2.3.2. Drought identification

The spatial-temporal drought characteristics for each grid are investigated based on the broadly used run theory method proposed by Yevjevich (1969). Following run theory, the condition with continuous SPEI values ≤ −1 for at least three consecutive months is considered one drought event in this paper. Next, drought frequency (DF) was measured as the number of drought occurrences per year. Similarly, drought area (DA) was estimated as the highest portion (number) of grids under dryness conditions for a period of time, which can be documented as a proportion (%) of the entire grid numbers across the selected region. The detailed calculation process can be found in the study of Guo et al. (2018).

2.3.3. Estimation of the exposed population

According to the United Nations International Strategy for Disaster Reduction (UNISDR, 2017), population exposure to drought is defined as the number of people in a drought-prone area. Population exposure can be measured by multiplying the anticipated drought frequency by the number of people under drought conditions (Jones et al., 2015; UNISDR, 2017). This research combined the projected population under five SSPs with the corresponding SSP-RCP climate change scenarios: SSP1 with SSP1–2.6; SSP2 with SSP2–4.5; SSP3 with SSP3–7.0; and SSP5 combined with the SSP5–8.5 scenario.

2.3.4. Causal factors in exposure change

Jones et al. (2015) stated that the changes in population exposure are mostly influenced by three factors: population factors (i.e., population change with time), climatic factors (e.g., drought frequency change with time), and population-climate interaction factors (e.g., both population and climate change with time). The decomposition for changes in population exposure is calculated by using the following equation:

$$\Delta D = X_j \times Y_j - X_i \times Y_i = X_i \times \Delta Y + \Delta X \times Y_i + \Delta X \times \Delta Y \quad (3)$$

where ΔD=total change in exposure; X_i = population level in period i; Y_i = drought frequency in period i; X_j = population level in period j; Y_j = drought frequency in period j;ΔX=population change from time period i to j;ΔY= changes in drought frequency from period i to j; $Y_i+\Delta X$ = population change effect; $X_i\times\Delta Y$=climate change effect; and $\Delta X\times\Delta Y$ = population-climate interaction. Then, the individual contribution of each factor is computed based on:

$$CFR_{pop} = \frac{Y_i + \Delta X}{X_i \times \Delta Y + \Delta X \times Y_i + \Delta X \times \Delta Y} \times 100\% \quad (4)$$

$$CFR_{cli} = \frac{X_i \times \Delta Y}{X_i \times \Delta Y + \Delta X \times Y_i + \Delta X \times \Delta Y} \times 100\% \quad (5)$$

$$CFR_{pop-cli} = \frac{\Delta X \times \Delta Y}{X_i \times \Delta Y + \Delta X \times Y_i + \Delta X \times \Delta Y} \times 100\% \quad (6)$$

where CFR_{pop} represents the contribution rate of the population change effect; CFR_{cli} represents the contribution rate of the climate change effect; and $CFR_{pop-cli}$ represents the contribution rate of the population-climate interaction effect.

3. Results

3.1. Model performance evaluation

It has been recognized that the evaluation of GCM capability in reproducing climatological variables provides a confident basis for future climate projections. In this study, the performances of 20 individual GCMs as well as their ensemble medians were evaluated considering the performances both before bias correction and after bias correction. The SPEI is regarded as the standardization of the difference between precipitation and PET. Therefore, GCM capabilities are appraised against ISIMIP observation data in terms of simulating precipitation and potential evapotranspiration (PET) across South Asia during the reference period (1995–2014).

Taylor analysis is broadly recognized to evaluate the performance of GCMs against reference data. In this study, the Taylor diagram was used to distinguish well-simulated GCMs in reproducing precipitation and PET over South Asia for further analysis. The results for precipitation are presented in Fig. 3a. The figure shows that before bias correction, most of the models had standardized deviations (SDs) varying from 0.6 to 1.2, while all the individual models after bias correction represented

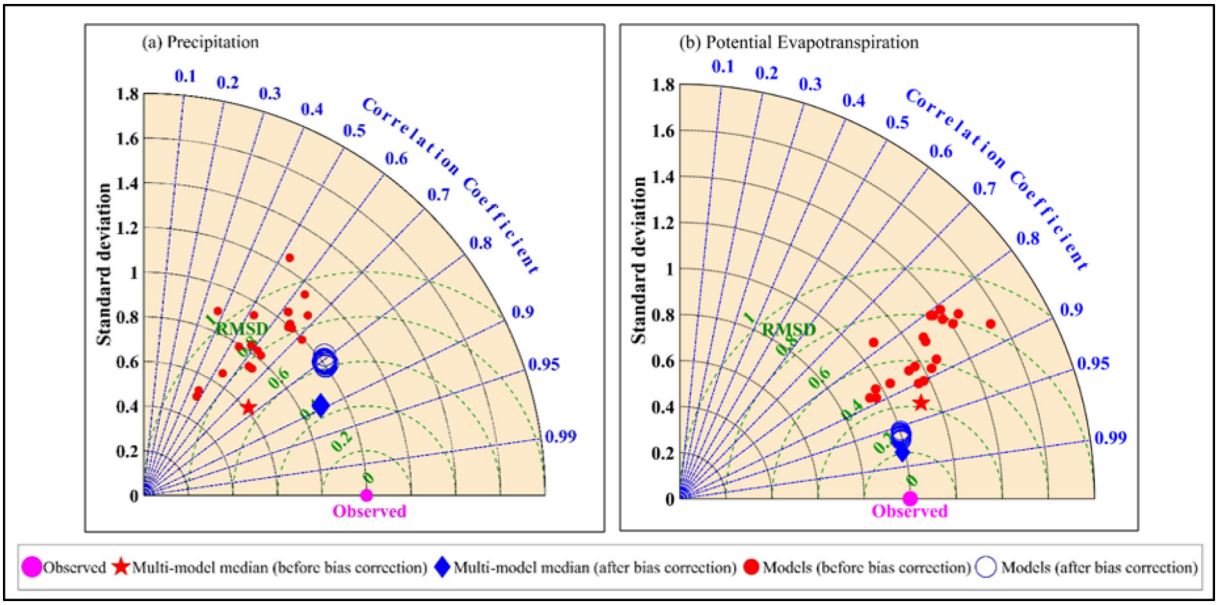

Fig. 3. Taylor diagrams of the simulated (a) precipitation and (b) potential evapotranspiration by 20 GCMs across South Asia for the period of 1995–2014 with ISIMIP as the observed data.

concentrated patterns laying closer to the standard deviation line of the observed data. Furthermore, correlation coefficients (CC) between the 20 GCMs and observed data ranged from 0.4 to 0.7 (before bias correction) with root mean square deviation (RMSD) ranging from 0.7 to 0.9, whereas after bias correction, CC reached ±0.8 and reduced the RMSD value by ~0.4. Furthermore, all the individual models and ensemble medians exhibited an improved capability in reproducing PET (Fig. 3b) over South Asia when compared to precipitation. Most of the models (before bias correction) simulated PET with a large SD relative to the observations (extent from 0.8 to 1.4) and an improved CC (0.8 to 0.9), whereas after bias correction, most of the models were simulated with a SD that was almost similar to that observed, with a concrete CC (≥0.95) and low RMSD. The multi-model ensemble (MME) median (both before bias correction and after bias correction) showed a stronger capability in simulating both precipitation and PET than the individual model, ensuring a high CC and low RMSD and standardized deviation near the observed data. Surprisingly, the ensemble median for precipitation simulation delineated small deviations in magnitude, which implies that GCMs have systematically underestimated precipitation distributions in South Asia. The bias-corrected individual GCMs and their ensemble medians provide better performance than before bias correction.

3.2. Anticipated changes in key climate variables

Generally, drought events are enhanced by rainfall deficits and continuous temperature increases as well as increasing evaporative demand. Future annual mean precipitation and PET changes under the SSP-RCP scenarios during the reference period (1995–2014) and projected period (2015–2100) indicating three defined periods, near-term period (2021–2040), mid-term period (2041–2060), and long-term period (2081–2100), are presented in Fig. 4. Overall, both the precipitation (Fig. 4a) and PET (Fig. 4b) show an increasing tendency under all the SSP-RCP scenarios across South Asia in the long-term period. The variations in terms of increases among scenarios are significant towards the long-term period. In the 2021–2040 period, the highest relative increases in precipitation and PET (relative to the reference period) are estimated to be ~4% and 1.9%, respectively, under SSP1–2.6. The lowest precipitation will be under SSP2–4.5 (0.1%). Furthermore, in relative terms, both the precipitation and PET are projected to increase under all scenarios during the mid-term period as well as the long-term period. In the mid-term period, the highest increases in annual precipitation and PET will be 6.3% and 4.2%, respectively, under SSP5–8.5, whereas the lowest precipitation (3.6%) is estimated to increase under SSP3–7.0. Likewise, in the long term, the greatest increases in annual precipitation and PET will be 23.1% and 10.8%, respectively, under SSP5–8.5, where the lowest rainfall is estimated under the lowest emission scenario SSP1–2.6. However, the changes in precipitation and PET are weaker in the 2021–2040 period and stronger in the 2081–2100 period for all scenarios.

3.3. Projected changes in SPEI, soil moisture and runoff

The included soil moisture and runoff variables in this study taken directly from similar models (20 GCMs) with the SPEI calculation. The SPEI has been compared with soil moisture and runoff diagnostics to demonstrate that the SPEI calculations here accurately reflect the drought responses within these coupled models. The geographical

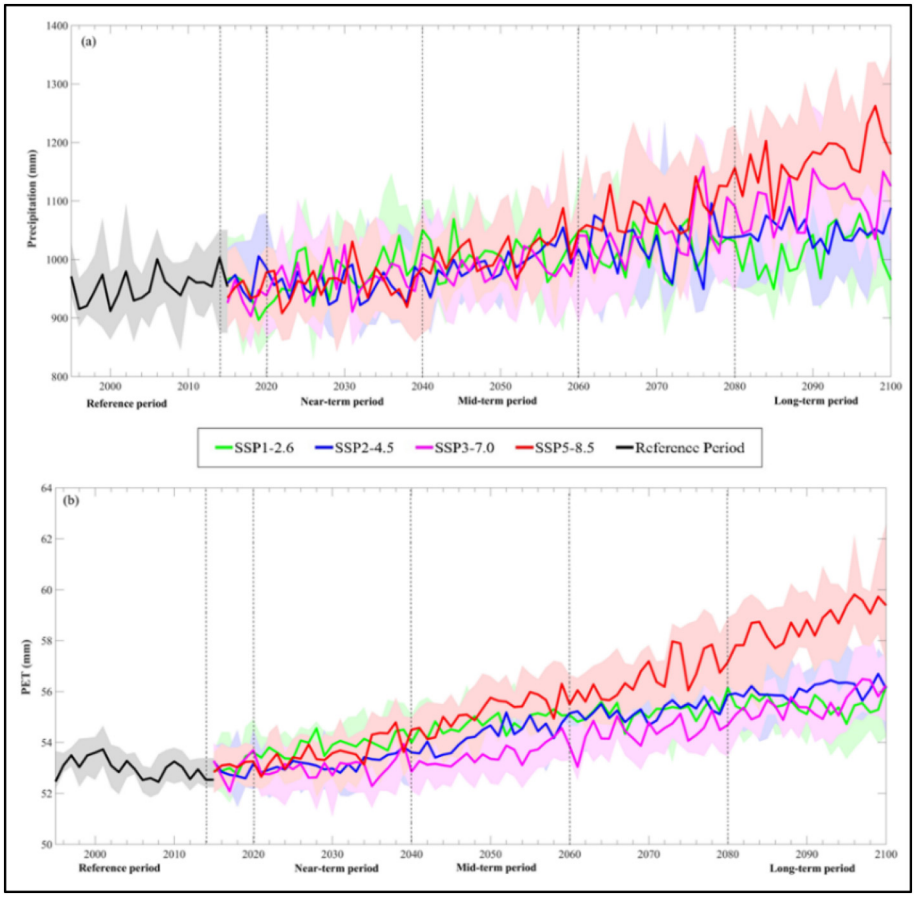

Fig. 4. Anticipated changes in precipitation and potential evapotranspiration for the 1995–2014 period and future period (2015–2100) under four SSP-RCP scenarios across South Asia: vertical dotted lines indicate different defined periods; solid-coloured lines are the MME median value, and shaded colours signify the 25th percentile and 75th percentile as the lower and upper limits of the GCMs, respectively.

structures of the future changes in surface soil moisture content, surface runoff, and SPEI for the long-term period are presented in Fig. 5. As significant changes and large variations in climatological parameters over South Asia exist in the long-term period (Fig. 4), the study analysed soil moisture and runoff for this period to demonstrate that the SPEI in this study accurately reflects the drought responses within the same GCMs. The figures illustrate decreases in soil moisture (Fig. 5A) and runoff (Fig. 5B) across the western part mostly in Afghanistan as well as the northern part (Nepal, Bhutan, and Bangladesh) under all scenario combinations. Notably, the magnitude of decreasing soil moisture and runoff are projected to become stronger over the western part from the low emissions scenario (SSP1–2.6) to the high emissions scenario (SSP5–8.5). Simultaneously, the increases in both soil moisture and runoff became pronounced in terms of magnitude and spatial extent over the eastern part of South Asia (India, Sri Lanka, and part of Pakistan) with increasing emission levels. However, the drying tendency in the soil moisture and runoff fields was largely captured by the SPEI (Fig. 5C) calculated using the same GCM climatological variables. In accordance with Fig. 5A, B, and C, it is obvious that dryness will be prominent in western South Asia under all emission scenarios. Though the soil moisture and runoff present consistency with SPEI here, results may be associated with some unavoidable uncertainties. The soil moisture and runoff data are not bias-corrected, which may exert interannual, seasonal and long-term trends. The relative changes are estimated for only the long-term period, so spatial discern in the near-tern and mid-term remain unclear. Furthermore, some individual models may have large overestimations or underestimations in some areas, which are not considered. However, although the multi-model ensemble method are used to reduce uncertainties, some uncertainties may remain for extreme values. However, the demonstrated spatial patterns of dryness and wetness trends (in Fig. 5A, B and C) are strongly consistent with the findings across South Asia reported by Zhai et al. (2020).

3.4. Drought frequency and area changes

The drought frequencies under the four SSP-RCP scenarios are presented in Fig. 6 for the target periods. During the 1995–2014 period, the drought frequency per year was 4.9 times across South Asia. For the future, the highest drought frequencies are projected to be 8.1

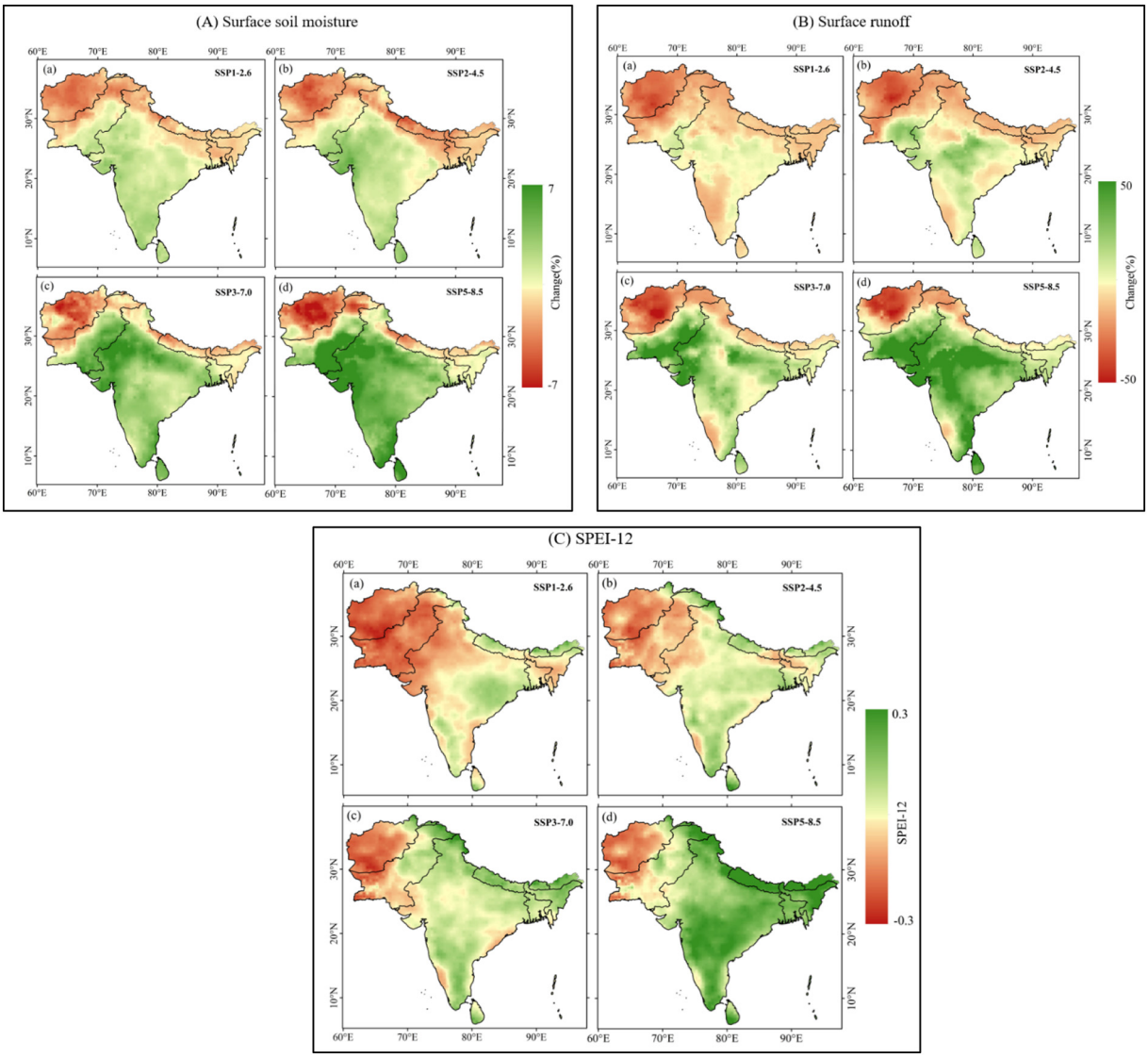

Fig. 5. Projected changes in surface soil moisture, surface runoff, and SPEI under four SSP-RCP scenarios across South Asia for the long-term period (2081–2100); (A) surface soil moisture and (B) surface runoff epitomize the percentage of changes during the long-term period (2081–2100) relative to the 1995–2014 period, and (C) SPEI-12 denotes the average over 2081–2100 estimated using the multi-model median value.

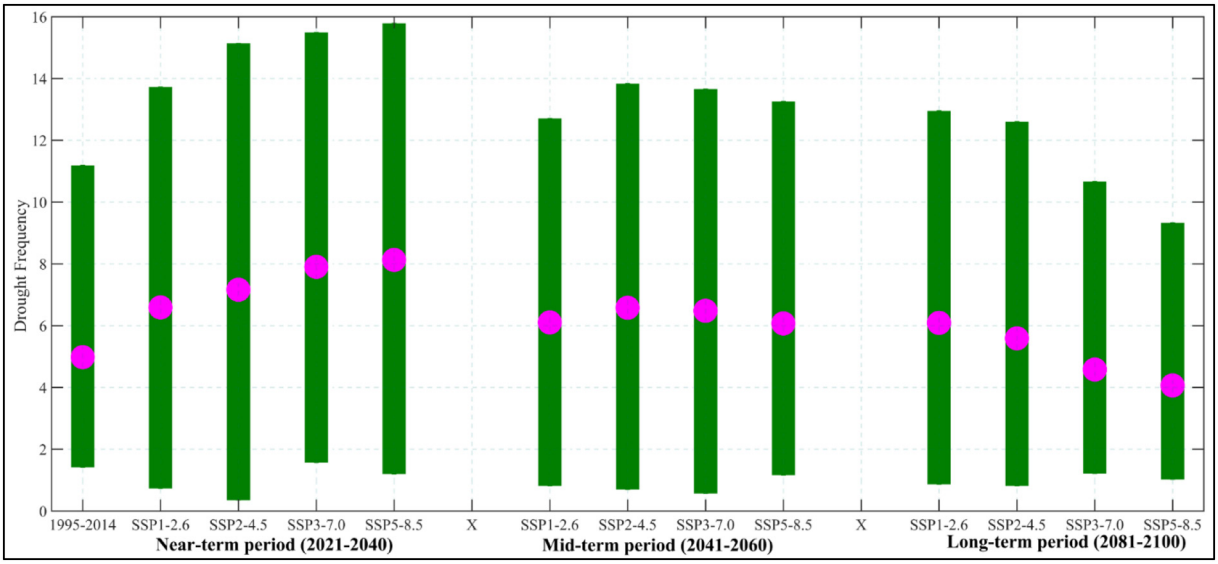

Fig. 6. Drought frequency for the reference period (1995–2014) and three future periods (2021–2040, 2041–2060, and 2081–2100) under four SSP-RCP scenarios in South Asia, where the coloured filled circles represent the MME median value, and the lower and upper limits of the green straight lines signify the 25th percentile and 75th percentile of the GCMs, respectively.

(SSP5–8.5), 6.6 (SSP2–4.5), and 6.1 (SSP1–2.6) times per year for the 2021–2040, 2041–2060, and 2081–2100 periods, respectively (Fig. 4). In the 2021–2040 period, the projected drought frequency increases from the lower forcing (SSP1–2.6) to higher forcing scenarios (SSP5–8.5). With regard to the reference period, the drought frequency in the near-term period will increase by 32.3%, 43.8%, 58.7%, and 63.2% for SSP1–2.6 to SSP5–8.5, respectively. During the mid-term period, the highest increase in drought frequency was 32.1% under SSP2–4.5. In the 2081–2100 period, the frequency significantly increases by 22.3% under SSP1–2.6. In summary, drought events in South Asia will become more frequent in the near future and will substantially decrease over long-term periods. Notably, more frequent drought events are anticipated with the higher forcing scenarios in the near-term period, while drought frequency in the long-term period will increase under lower emission scenarios.

The horizontal pattern of frequent drought events (DF) in the reference period (1995–2014) and relative changes for the three defined time horizons across South Asia are shown in Fig. 7. In the 20 years of the past period (1995–2014), South Asia faced substantial drought events 5 times per year, which occurred mostly over India (central, western, and north-eastern parts) as well as Bangladesh, part of Nepal, Bhutan, and Afghanistan (Fig. 7a). Moreover, drought frequencies ≥6 times were pronounced in western South Asia (mostly Pakistan and extended to Afghanistan), and drought events of more than 6 times per year were striking across the south-eastern warm humid region of India and Sri Lanka. A pronounced pattern of drought frequency is exhibited in the near-term period (Fig. 7b, e, h, k). With regard to the reference period, drought events in the near-term period are projected to become 60% higher over almost all of South Asia. Drought events will be aggravated to more than 60% higher than the reference period across the eastern state of India, central and western India, and part of Bangladesh and Nepal under all scenarios. However, in the mid-term period (Fig. 7c, f, i, h), drought frequency will increase by 60%, mostly in central and western India, the eastern state of India, and part of Pakistan and Afghanistan. In this period, drought events tend to decrease across the south-eastern warm humid region of India and northern Pakistan. Surprisingly, a pronounced decreasing (70%) pattern is projected in the long-term period (Fig. 7d, g, j, l) under all scenarios. In this period, drought frequency will decrease mostly in the eastern part, while increased DF is distributed in the western part (mostly Pakistan and Afghanistan) under all scenario combinations. In the long-term period, the dominant decreasing pattern in DF is exhibited across the central and eastern parts of South Asia (India, Sri Lanka, Nepal, Bhutan, and Bangladesh) under SSP5–8.5 and SSP3–7.0. In conclusion, drought is projected to become weaker in the long-term period. A strong spatial pattern of DF in the near-term period is inclined to increase towards higher emission scenario combinations; in contrast, the opposite pattern is observed in the long-term period.

Fig. 8 represents the areal coverage of drought events for the 1995–2014 period and three future periods under four emission scenarios in South Asia. In the reference period, the annual drought-affected area was 12.4% of the total area. During 2021–2040, the projected areal coverage will increase under all emission scenarios. Under the SSP5–8.5 and SSP2–4.5 scenarios, the annual affected areal coverage will be 18.3% of the total area at the highest and 17.2% at the lowest area, respectively. In 2041–2060, the highest areal coverage accounts for 15.9% under the SSP3–7.0 scenario. In the long-term period, the percentage of affected area decreases under SSP3–7.0 and SSP5–8.5 compared to the reference period. Relative to the reference period, drought area is projected to decrease the most by 62.1% under SSP5–8.5 and increase by 41.3% under the lowest emission scenario (SSP1–2.6). In summary, the percentage of affected area increases is strongest during the near-term period, which further intends to decrease towards long-term periods. The drought-affected area in the long-term period will largely decrease towards higher emission scenarios.

3.5. Projected changes in population exposure and contributing factors to exposure changes

To ascertain the prospective drought impacts on South Asia, drought-induced population exposure and the role of associated contribution factors under four SSP-RCP scenarios for the three future periods and reference period are presented in Fig. 9. The population exposed to drought in the 1995–2014 period was 384 million, which is 24.2% of the total population. The multi-model scenario-based analysis shows that the population exposed to drought will increase across South Asia for the three future periods compared to the reference period. Except for SSP5–8.5 in the long-term period, the exposed population will increase under all scenario combinations. In 2021–2040, population exposure is

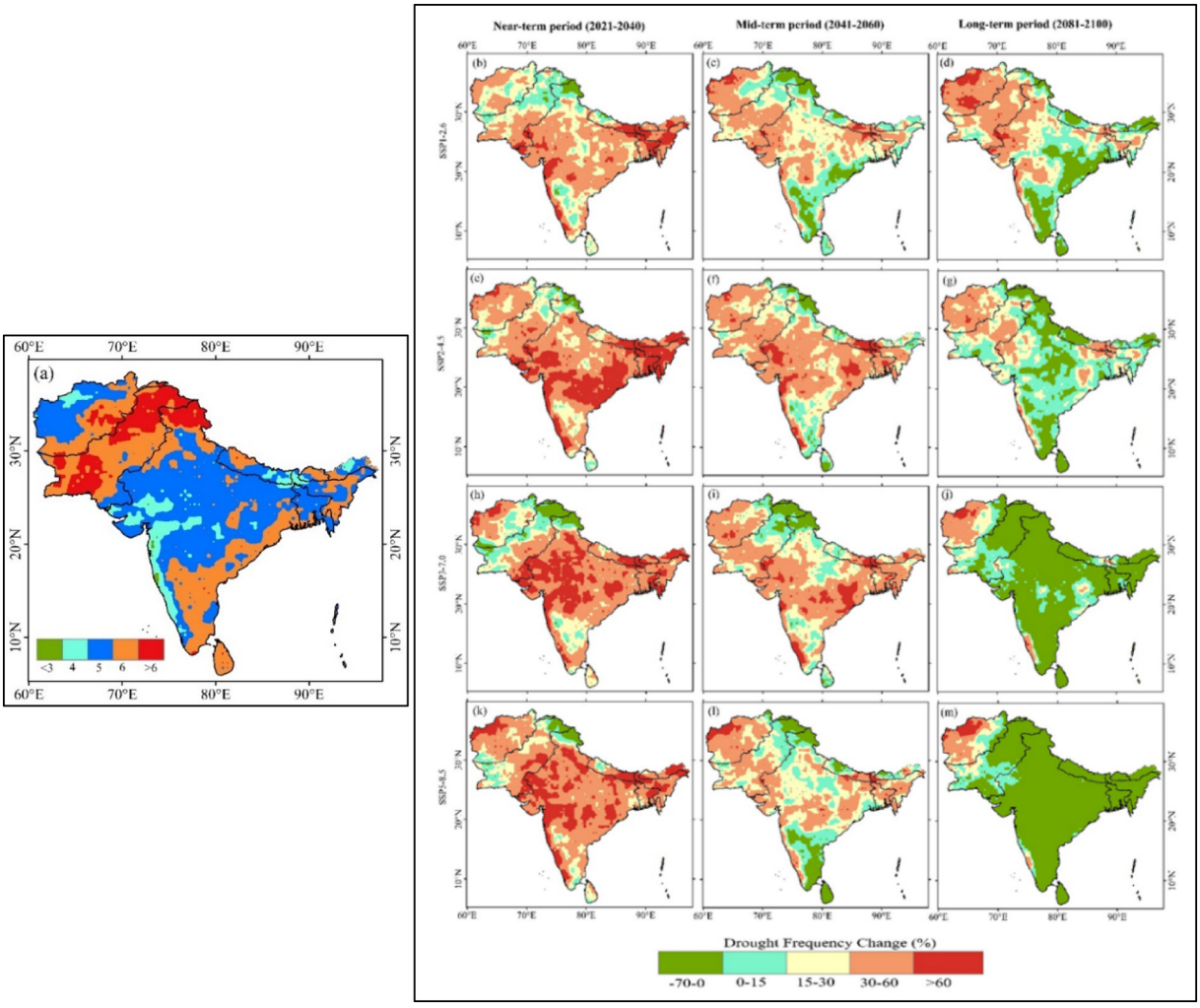

Fig. 7. Spatial distribution of drought frequency under four SSP-RCP scenarios in South Asia: (a) for the reference period (1995–2014) and (b–m) future changes for three periods (2021–2040, 2041–2060, and 2081–2100) relative to the reference period.

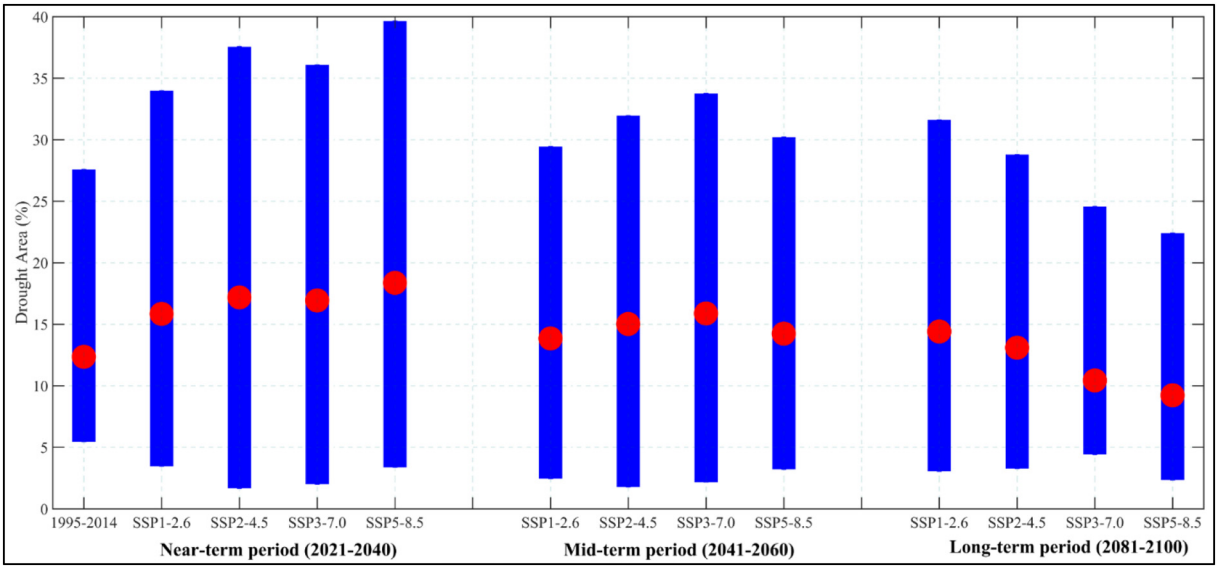

Fig. 8. Drought areal coverage for the reference period (1995–2014) and three future periods (2021–2040, 2041–2060, and 2081–2100) under four SSP-RCP scenarios in South Asia, where the red circles are the MME median values, and the lower and upper limits of the straight blue lines signify the 25th percentiles and 75th percentiles of GCMs, respectively.

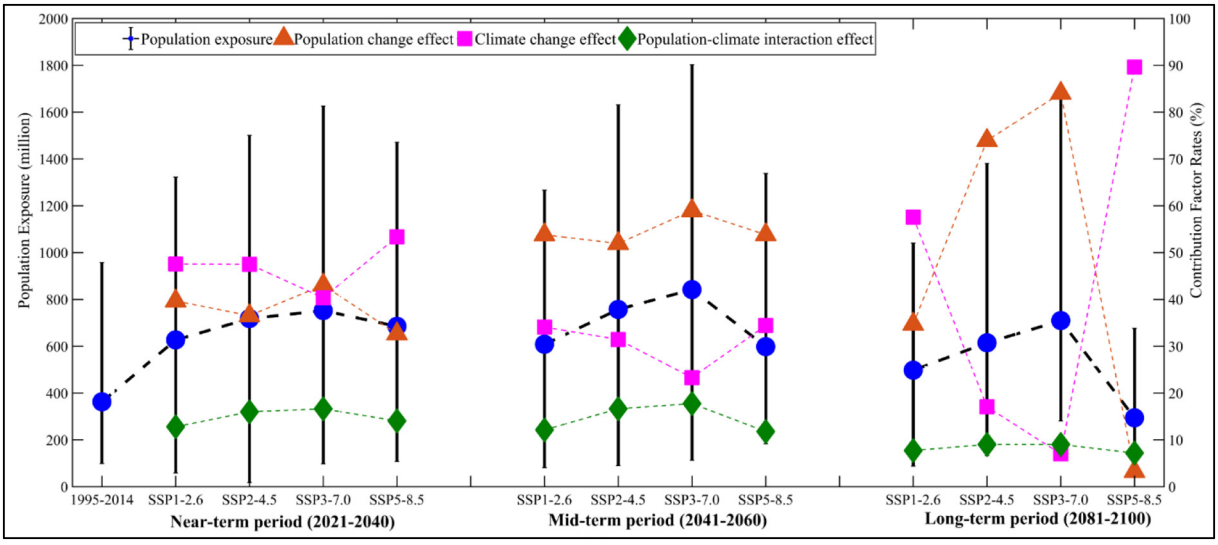

Fig. 9. Average monthly population exposed to drought (blue circle, primary y-axis) and contribution of driving forces to exposure changes (pink square, yellow triangle (top) and green diamond shapes, secondary y-axis) for the reference period (1995–2014) and three future periods (2021–2040, 2041–2060 and 2081–2100) under four SSP-RCP scenarios in South Asia; where the filled coloured square, circle, triangle (top) and diamond shapes signify the MME median value; and the lower and upper limit of the black straight lines denote the 25th and 75th percentile of the GCMs, respectively.

predicted to be 1.7-, 1.9-, 2.0-, and 1.8-fold higher than the reference period under SSP1–2.6 to SSP5–8.5, respectively. During the mid-term period, higher population exposure is estimated to increase approximately 2.1- and 2.3-fold under SSP2–4.5 and SSP3–7.0, respectively, where the lowest exposure (1.6-fold) is recorded under the SSP5–8.5 scenario. In this period, the population exposed to drought peaked under all scenario combinations except SSP5–8.5. In the long-term period, population exposure to drought is comparatively weaker than that in earlier periods. Surprisingly, the 2081–2100 exposure decreased by 18.8% relative to the reference period under SSP5–8.5. Exposure is projected to increase to 1.9-fold higher than the reference period under the SSP3–7.0 scenario. In this period, population exposure increased under a strongly fragmented pathway (SSP3) and decreased in the growth-oriented world, securing both high forcing levels. It can be concluded that the overall projected change in exposed people will be strongest from the early part of the century to the middle of the century and then gradually become weaker until the far future under all scenario combinations. Notably, the higher exposure (2.1-, 2.3-, and 1.9-fold, respectively) was estimated under the worst-case scenario SSP3–7.0 for all three periods, where the greatest increase was recorded at 132.2% (2.3-fold) in the middle of the century with regard to the reference period. In contrast, the largest decreasing exposure (18.8%) is projected under SSP5–8.5 in the long-term period.

Furthermore, to assess the contribution of decomposition factors to changing population exposure over South Asia in terms of the population change effect, the climate change effect and population-climate interaction change effect are illustrated in Fig. 9 (secondary y-axis). For three targeted time horizons, under different scenario combinations, the effects of population change and climate change are the main contributors, while the effect of population-climate interaction is never considered to be high in terms of exposure changes. In 2021–2041, the climate change effect will have the largest contribution to changing population exposure for all scenarios except SSP3–7.0. The highest contribution is estimated to be almost 53.3% under SSP5–8.5, while the population change effect reaches 43.0% under SSP3–7.0. During the mid-term period, the population change effect will be the prime factor for population exposure changes under all scenarios, where the population change effect is estimated to be 58.9% at the highest under SSP3–7.0, whereas the climate change effect will contribute 34.4% under the high emission scenarios (SSP5–8.5). In 2081–2100, the population change effect will be dominant under SSP2–4.5 and SSP3–7.0, while the climate change effect will be the main contributor under SSP1–2.6 and SSP5–8.5. In this time horizon, the climate change effect will have the greatest contribution up to 89.6% under SSP5–8.5, and the population change effect will reach ~84% for SSP3–7.0.

To further examine the geographic structure of the exposed population during 1995–2014 and the future, the changes under three periods relative to 1995–2014 in South Asia are shown in Fig. 10. Population exposure in the reference period (Fig. 10a) was an average of 1297 per km^2 across South Asian countries. Population exposure was comparatively low in the western part (Afghanistan as well as the western part of Pakistan) but high in the northern and south-eastern parts of South Asia. Population exposure >1000 per km^2 is estimated mostly across the Indo-Gangetic Plain region. In the reference period, exposure is pronounced over major populous cities, namely, Mumbai, Delhi, Bangalore, Hyderabad, Ahmedabad of India; Karachi, Lahore, Faisalabad of Pakistan; Colombo of Sri Lanka, and throughout Bangladesh.

To refine the spatial distribution for the future periods, the results show that exposed people are pronounced mostly over India due to the country being highly populated as well as the more frequent drought events. In the near-term period (2021–2040) (Fig. 10b, e, h, and k), population exposure to drought is expected to increase by ≥150% compared to that in 1995–2014, mostly across the central and eastern states of India, as well as part of Nepal and Bangladesh under SSP3–7.0 and SSP2–4.5. Furthermore, the number of exposed people will increase by 120% under SSP5–8.5 across the western, central, and eastern states of India, while the lowest increase (50%–80%) is mainly exhibited under the low emission scenario SSP1–2.6 over similar areas and extends to Pakistan and Afghanistan. Likewise, in the middle of the century (Fig. 10c, f, i, and l), the strongest pattern of increased exposure (≥150%) is observed under the SSP3–7.0 and SSP2–4.5 scenarios. The pronounced pattern is distributed over the large cities, namely, Mumbai, Ahmedabad, Pune, Hyderabad, Bengaluru, Kolkata, Delhi of India; Balochistan, Sindh, and Hyderabad of Pakistan; Herat of Afghanistan, Katmandu of Nepal, and Dhaka of Bangladesh SSP3–7.0.5, especially under SSP3–7.0. In this period, exposure is inclined to increase by 50%–

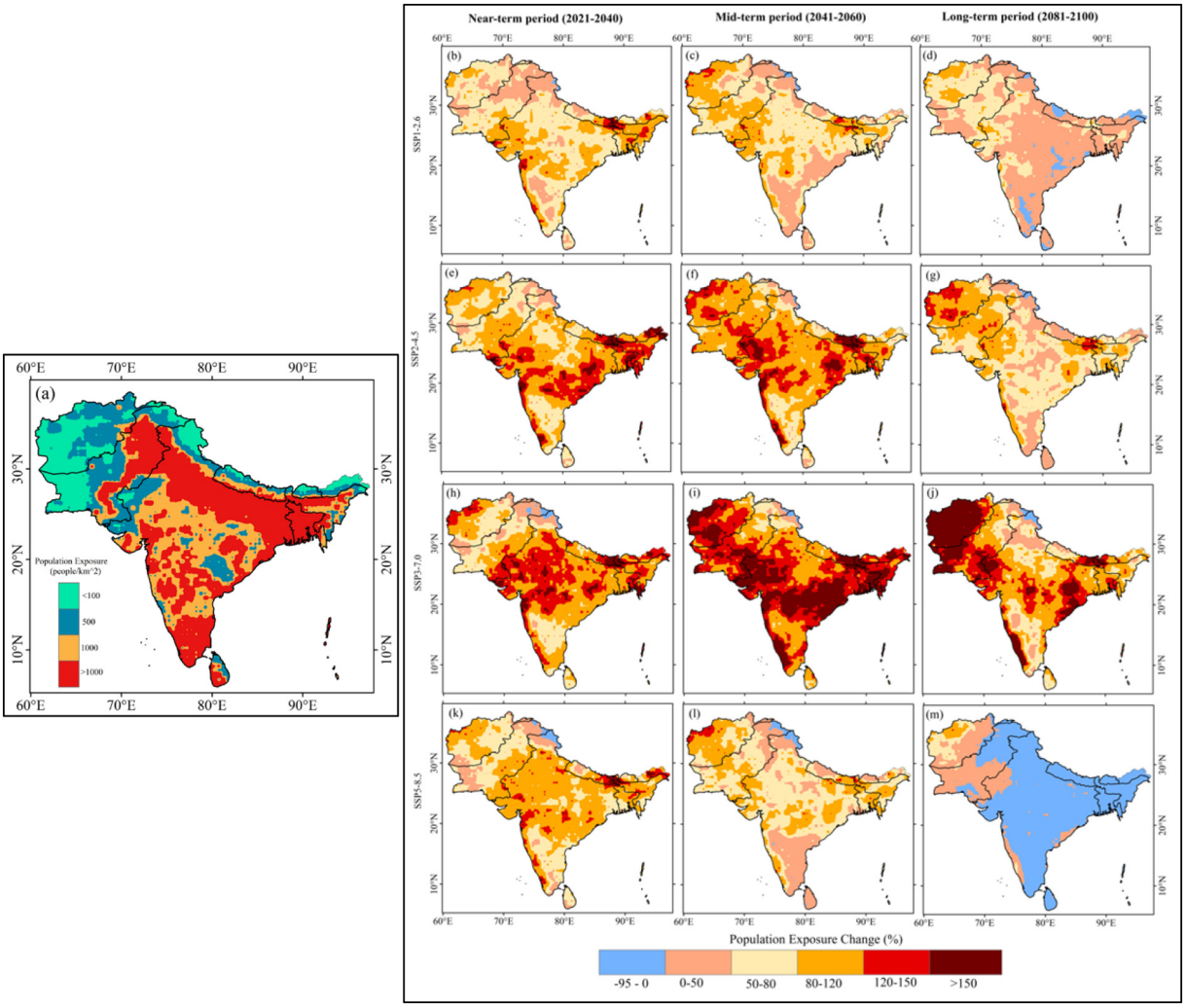

Fig. 10. Spatial distribution of population exposure under four SSP-RCP scenarios in South Asia: (a) for the reference period (1995–2014) and (b–m) future changes for three periods (2021–2040, 2041–2060, and 2081–2100) relative to the reference period.

80% for SSP5–8.5 and SSP1–2.6 across the eastern part of South Asia with an extended tendency to increase by 120%, mostly across Pakistan and Afghanistan. By the long-term period (Fig. 10d, g, j, and m), the largest increase in exposure (>150%) is estimated under SSP3–7.0, which is strongest across the western part of South Asia (mostly Afghanistan). In contrast, population exposure is anticipated to decrease greatly over the eastern part under SSP5–8.5. During this period, the western part (Pakistan and Afghanistan) exhibited an increase in exposure under all scenario combinations. Since the drought frequency and population growth (except SSP3) are projected to be lower in this period, the central and eastern parts of South Asia (India, Sri Lanka, Nepal, Bhutan, and Bangladesh) show a low or even high decreasing (≤95%) pattern under the higher emission scenario. In summary, in relative terms, the pronounced spatial distribution pattern largely exhibits an east-to-west shift from the near-term to long-term period. The highest increasing pattern is pronounced under high societal vulnerability with the medium to high forcing level scenario SSP3–7.0 (Fig. 10h, i, and j) for all the target periods. In terms of substantial increases, the geographical distribution of the exposed population is predicted to become even more pronounced over India, Afghanistan, Bangladesh, and part of Pakistan, especially under the worst-case scenarios (SSP3–7.0) in the middle of the century. Notably, exposure to drought is predicted to decrease significantly in India, Sri Lanka, Nepal, Bhutan, and Bangladesh for SSP5–8.5 in 2081–2100.

4. Discussion

This paper represents population exposure to drought as well as associated factors influencing exposure changes over time in South Asia. In this regard, 20 up-to-date GCM outputs under four SSP-RCP scenarios are explicitly used from the new-state-of-the-art CMIP6, and projected population data encapsulated under socio-economic scenarios (SSPs). To explore drought-induced population exposure throughout the 21st century, the SPEI-based drought frequency and affected area were predicted first, and finally, the impact of different causal factors on exposure changes was quantified.

Since CMIP6 is still in the incipient phase, all the essential variables are not available for all the GCMs under all designed scenarios. To date, 20 GCMs have been made available with all required variables (for this study) under four common SSPs-RCPs scenarios (SSP1–2.6, SSP2–4.5, SSP3–7.0, and SSP5–8.5) among these GCMs. In addition, the performance of the GCM evaluation against the observed dataset signifies that most of the selected models have good capability in capturing climate variability over South Asia. These findings suggest an added improvement in the horizontal resolution of CMIP6-GCMs. The enhanced performance of climate models can be influenced by high

horizontal resolution (Watterson et al., 2014). Therefore, in relative terms, the improved performance of GCMs in apprehending climate parameters and drought characteristics is likely associated with the boosted representation of physical processes in the CMIP6 climate models. Advances in the representation of physical processes have been made in GCMs from CMIP6, as also reported by some previous studies (Di Luca et al., 2020; Xin et al., 2020; McKenna et al., 2020; Su et al., 2020). Therefore, the selected 20 high-resolution global climate models with four common SSP-RCP scenarios are considered for further analysis. Next, it has been recognized that the multi-model ensemble provides a reliable estimation for scenario-based studies instead of using an individual model's output. In this study, the evaluation results indicate that the multi-model ensemble (MME) median securing bias correction provides better representativeness than an individual model. Similarly, Pierce et al. (2009) stated that the multi-model ensemble depicts an improved overview of regional climate change compared to an individual model by reducing the spatial ambiguity and inconsistency.

To determine the magnitude of the changes to the exposed population over time, a reasonable reflection of drought is a prime concern. In this study, the multi-model simulated soil moisture, runoff, and drought indices (SPEIs) predicted increased drought risk with similar spatial distributions in South Asia. These comprehensive analyses suggest an obvious drought conditions in the western part of South Asia, whereas the eastern part will face extreme wetness conditions (which might result in flooding). This findings strongly corroborate the statement by Schleussner et al. (2018) that one part of the climate hotspot of South Asia will face acute drought conditions, while the opposite area will be flooded by the 21st century. Therefore, the anticipated drought reflection in South Asia calculated by using the SPEI index can be considered an accurate demonstration within these included GCMs with decreased uncertainty and variability.

The anticipation of population exposure to drought under a changing climate signifies the rapidity of the human system being jeopardized by hazards. Drought-induced population exposure is interconnected with its occurrence, area coverage, and intensity as well as the spatio-temporal distribution of the population. However, population exposure to drought in South Asia is predicted to become greater than that in the current period due to the more frequent occurrence of drought events with extended areal coverage as well as the level of population growth. Among the three target periods, this study discerns a stronger escalation in drought occurrence with a higher percentage of area coverage in the near-term period (2021–2040) and a further tendency to diminish on the road to a long-term period. Likewise, the exposed population is inclined to be dominant in the near-term as well as mid-term periods but drastically reduced onwards at the end of the century (2081–2100). This result is an indication of concrete uniformity and interconnection among the findings in terms of both quantitative estimation and spatial distribution. The new generation of climate models from CMIP6 can increase the confidence in projecting strong exposure changes under all the scenarios. Considering the high confidence, policy makers should make efforts to enhance resilience and adapt to growing exposure as well as the proper provision of migration systems throughout the coming 20–40 years. However, the findings of this study corroborate those of some previous studies. The CMIP5-based study by Wang et al. (2020) reported enlarged exposure to drought in the Indus River Basin of South Asia for 2021–2065. In the 2020–2039 period, the people exposed to drought are predicted to increase compared to the historical period (Wen et al., 2019). Similarly, Chen et al. (2018) reported that moderate drought will be aggravated in China through the 2020–2039 period, resulted in the largest affected population. Notably, an unavoidable increase in population exposure to drought is predicted to occur over South Asia by the early and middle of the century.

It can be highlighted that our study demonstrates a stronger increase in drought frequency in the near-term period than in the long-term period. This result could be due to lowering precipitation and PET estimated in the near-term period across South Asia, while excessive precipitation and PET are anticipated by the end of the century, especially under the high forcing levels. A great increase in precipitation is predicted for SSP5–8.5 in the study area by the 21st century (Almazroui et al., 2020; Zhai et al., 2020). In general, drought events with short durations are more frequent in occurrence, while long-term droughts occur less frequently. In addition, decreasing precipitation influences short-term drought occurrence, and a large evaporative demand leads to long-term events. High evaporation contributes to a decline in surface runoff and soil moisture, which augments drought persistence significantly compared to precipitation (Sun et al., 2017). Furthermore, many studies using CMIP5 reported that the frequency and level of intensity of drought will be intensified with increasing global temperatures (Cook et al., 2018; Smirnov et al., 2016; Su et al., 2018; Lin et al., 2020). However, Lehner et al. (2017) stated that the risks of drought and temperature increases do not always follow any simple linear relationship. Miao et al. (2020) mentioned that dryness conditions across Asian drylands are projected to worsen at 1.5 °C compared to 2.0 °C, which signifies that an increase in global temperature would not lead to drought escalation. As drought is controlled by different components of the hydrological cycle (precipitation, evaporation, runoff, etc.), the risks, degree, intensity, duration and effects of drought vary by region. Nonetheless, a recent study using CMIP6 stated that the near future period can be considered a drought-prone period for India (Shrestha et al., 2020). A CMIP6-based study in South Asia by Zhai et al. (2020) found that drought events will become even more frequent under a low emission scenario (SSP1–2.6) than under a high emission scenario (SSP5–8.5). In the near-term period, drought events will be triggered by decreasing precipitation, whereas drought occurrence in the long-term period will be reduced by the alleviating response of heavy rainfall, especially for high emission scenarios. Furthermore, as PET is inclined to increase largely in the long-term period, drought events will occur with longer durations but less frequently. It is apparent that future drought escalation in South Asia will lead to increased evaporative demand. Therefore, it must be suggested to use PET-based drought indices to reflect the actual drought conditions in South Asia. Significant changes in South Asian climate parameters will be contributed by high greenhouse gas (GHG) emissions, since large increases in PET and precipitation are anticipated to increase under the scenarios with high mitigation challenges and low adaptation challenges (SSP5–8.5) in the long-term period. The latest study using CMIP6 by Ha et al. (2020) also reported that heavy precipitation and large PET will increase over Asia, where PET is offset by precipitation in India. Since both PET and precipitation are predicted to increase under SSP-RCP scenarios, considering the ratio of PET and precipitation, drought might become worse in the future due to evaporative demand (Jiang et al., 2020a).

This study reveals that the effects of precipitation and PET on dryness/wetness trends are significant from a long-term perspective (2081–2100) (Table S2). The process of dry events (drought) was originally accelerated by the decrease in precipitation in the early stage. Trenberth et al. (2013) also stated that warming-induced drought events may have been accelerated and worsened due to a lack of precipitation in the early part of the century. However, with regard to relative changes, precipitation increases faster than PET (wet conditions) in the long-term period. The probability of the area affected by wet events (floods) is higher in this period, especially under high emission scenarios. The region will be wetter in the far future; the increase in P-PET is induced by a substantial increase in precipitation (relative to the historical period). Precipitation increases of ≥10% contribute to a decrease in extent of the drought frequency increase (Table S2). When the increase in precipitation reaches 15%, the drought frequency decreases ~8% under SSP3–7.0. Similarly, the chances of the occurrence of extreme wet events (flood) were augmented (drought frequency decline ~18%) when precipitation was inclined to increase by >20%. Therefore, it is obvious that extreme wetness events (floods) across some regions of

South Asia could be triggered due to an excessive increase in precipitation at the end of the century. Consequently, population exposure to drought is projected to decrease (Fig. 9). Nath et al. (2017) also stated that the Indo-Gangetic region of South Asia will be affected by wet events (floods) in the long-term period due to excessive rain. However, the precipitation effects on regional dryness and wetness trends are interlinked not only to the precipitation amount but also to the aggregation extent, frequency, and intensity of the precipitation. The greater the precipitation concentration, the more chances to accelerate extreme wet events.

Furthermore, recognizing the significance of various decomposition factors (i.e., climate change effect, population change effect, and interaction effect) on exposure changes provides a pivotal basis for initiating policy responses to reduce the number of South Asian people exposed to drought. In the near-term period, the climate change effect is found to become a pivotal causal factor in exposure changes across South Asia, as the occurrence of drought events with a large affected area is predicted to trigger more rapid exposure with time. During this period, population growth is considered to be sluggish, while the climate change effect contributes largely to shaping the future level of exposure to increase under all emission scenarios except SSP3–7.0. Hence, it is obvious that compared to future population changes, estimated exposure will be most sensitive to future GHG (mainly CO_2) concentration changes during the early part of the century. In contrast, the effect of demographic changes on exposure changes is significant for the mid-term period under all emission scenarios. In this period, population growth is estimated to peak under all scenarios, especially the high societal vulnerability scenario SSP3. Future changes in climate during the mid-term period play a minor role in explaining exposure changes over South Asia. Furthermore, in the long-term period, the effect of population changes is the primary contributor under SSP2–4.5 and SSP3–7.0, whereas the climate change effect is dominant under the SSP1–2.6 and SSP5–8.5 scenarios. Interestingly, in the long-term period, population exposure is projected to decrease under SSP5–8.5 due to a decrease in drought frequency. Gupta and Jain (2018) also reported that drought frequency in the far future will decrease under high emission scenarios (RCP8.5) across the eastern state of India, which is similar to our result. However, exposure changes in South Asia are mainly due to demographic changes. The demographic change effect is robust under SSP3–7.0 for all periods, as the highest number of people is projected to increase continually under the SSP3 scenarios in South Asia. The number of people exposed to drought is the largest under the SSP3–7.0 scenario as the combination of a relatively high societal vulnerability scenario (SSP3) with a high forcing level. SSP3 imposes high mitigation and adaptation challenges (O'Neill et al., 2017). Rapid population growth, highly unmitigated emissions, slow technological changes in the energy sector, low investment in human capital, high inequality, unfavourable institutional development, and a large number of people under climate change conditions would likely trigger a strong increase in vulnerable conditions for South Asian countries, worsening further drought impacts. The greatest drought-exposed population is estimated under the newly developed gap scenario SSP3–7.0, which was not possible by using previous CMIP5 scenario combinations. The consideration of a future 'plausible world' regional rivalry or fragmentation pathway-based forcing scenario is obvious for further study over South Asian countries. Generally, in South Asian countries, population growth is high, mainly in India, which is the second most populous country in the world with high density. In addition, some pivotal features of regional rivalry appear day by day among South Asian countries. Resurgent nationalism, regional conflicts and competitiveness, more focus on achieving energy and food security, slow economic development, increasing fossil fuel dependency, persistent inequalities, and border-based development issues are salient aspects of fragmentation in South Asia. Current border-based conflict along Indian borders with different neighbouring countries, such as Pakistan, China, Nepal and Bangladesh, is vibrant evidence. Therefore, low international priority for addressing environmental changes leads to strong climate change impacts on humans. However, this study highlights two key insights regarding policy interventions in South Asia: climate change mitigation and population growth control dimensions. The relation between these two components is vis-a-vis. The more population growth there is, the more anthropogenic climate change enhancement there is. In contrast, a changing climate aggravates population exposure to drought acutely, resulting in a dense population. Hence, additional attention should be urgently paid to formulate policies on climate change mitigation through GHG emissions cuts as well as population growth control to reduce future population exposure to drought in South Asia, focusing on India. The formulation of population and adaptation policies is urgent in South Asia to limit population growth and enhance adaptations to drought. Changes in population exposure are mainly influenced by the population change effect over Asia, focusing on India, China, and Bangladesh (Liao et al., 2019). However, Smirnov et al. (2016) reported that the overall condition of the changing climate is more responsible for population exposure to extreme drought across India, Bangladesh, and other South Asian countries under RCP4.5 and RCP8.5. This contradiction may be due to the new generation of GCM (CMIP6) outputs and different scenarios used in this study. On the other hand, exposure change is greatly driven by the climate change effect under SSP5–8.5 in all periods. Such a plausible outcome signifies the direct implications of climate mitigation policies to limit emissions. Furthermore, in terms of spatial coverage, the exposed population will be low in the high land (mountains) as well as desert areas but large in the plain and populous areas across South Asia. These changes are subjective to the overall major increase in exposed population numbers over the high population growth in India during the near-term to mid-term period. In contrast, the exposed population is anticipated to be pronounced in Afghanistan at the end of the century. Hence, additional concern must be given to monitoring in relation to future droughts in India and Afghanistan. Watts et al. (2015) also found similar findings that population exposure is low in mountainous regions but high in densely populated areas. Nonetheless, given the prior importance in the population change effect as well as the climate change effect as the key drivers of exposure changes, a substantial policy designed to reduce South Asian population exposure to drought must be needed to pay pivotal attention to socio-economic advancement and climate change mitigation efforts, especially for the near-term and mid-term periods of the century.

Dissecting the anticipated changes, it can be boldly written that not only will climatological drought increase across South Asia in the future but also extreme wet events (floods) will become probable at the end of the century. Extreme events, including droughts and floods, will become more common over South Asia due to increased variability in climate parameters (especially precipitation). In spatial terms, wetness is projected to increase across the eastern part of South Asia, but dryness will be sustained in the western part (Fig. 5). This study incorporated the impact of drought on South Asia in the future, while the results show that in the long term, the population may not be exposed to droughts (water shortage), and they may be exposed to floods and other natural disasters. As precipitation is projected to increase, it increases the risk of flooding in the study area and may cause immigration driven by climate change to the area, which adds uncertainty to the results of the study.

5. Conclusions

This work has explored the anticipated changes in the exposure of the South Asian population to drought with the contribution of decomposition factors to exposure changes under four of the latest CMIP6 scenarios for the three future periods (2021–2040, 2041–2060, and 2081–2100). The use of a bias-corrected MME median has enhanced the confidence in discerning drought events and exposure predictions over South Asia. The results show that the evaluation of precipitation and potential evapotranspiration (PET) shows that the CMIP6 model

ensemble is robust in simulating climate variables in South Asia. In addition, comprehensive analyses of soil moisture, runoff, and SPEI suggest actual representation of drought in South Asia within the selected GCMs.

The results of the study revealed that with the improvement in the spatial resolution in CMIP6-GCMs, the selected models performed well in capturing regional climate variables and accurately reflecting drought across South Asia. It is anticipated that both precipitation and PET will increase from 2021 to 2040 to 2081–2100 relative to the reference period. Furthermore, the study reveals that compared to 1995–2014, drought events and drought-affected areas escalated with higher emission scenarios, which were strongest in the near-term period and tended to decrease in the long-term period. Frequent drought events are pronounced in the central and south-eastern parts of India and Nepal in the near- and mid-term periods. In the long term, increasing frequency patterns dominated across the western part, especially in Pakistan and Afghanistan, but greatly decreased in the eastern part of South Asia. The overall projected increase in the number of exposed populations will be strongest (>1.5-fold) from the early century to the middle of the century and then gradually become weaker until the far future under all scenario combinations. Notably, the highest exposure (2.1-, 2.3-, and 1.9-fold) was estimated under the worst-case scenario SSP3–7.0 for all three periods, where the greatest increase was recorded at 132.2% (2.3-fold) in the middle of the century with regard to the reference period. In contrast, the largest decreasing exposure (18.8%) was projected under SSP5–8.5. In terms of geographic distribution, a significant increase in the number of people exposed to drought will be pronounced across India, especially in the near-term to mid-term period, while it will greatly shift towards the west (mostly Afghanistan) by the end of the 21st century. Finally, it was estimated that the two pivotal factors in population exposure changes are drought frequency and population change. Taking into account all the scenarios and time periods, the population change effect has a prime role in South Asian exposure changes; climate change has a further effect, and population-climate interaction has never the leading effect. The climate change effect is dominant in the near-term period, where the population change effect is prominent in the mid-term period. However, the climate change effect has a larger effect on exposure changes under SSP5–8.5, whereas the population change effect is greater under SSP3–7.0.

The limitations of this study include that in our analysis, this paper did not consider population patterns in rural-urban areas or demographic and socioeconomic characteristics of the population, such as age, gender, income, or level of education, which are considered to influence drought-related death or injury. Moreover, SSP-based projected global population data are widely used as the best high-resolution data, which has some uncertainties. The main uncertainty is derived from the assumption of demographic evolution. In SSP scenarios, population projections do not consider changes in the population policies of individual countries (i.e., two-child policy in China). Therefore, it is needed to consider this key population policy assumption in the simulation period data to secure the accuracy of the future risk assessment results. Moreover, warming-induced climate change leads to escalated drought frequency, whereas socioeconomic development enhances social awareness and capabilities to reduce disaster vulnerability. Population exposure to drought depends on both the hazards and regional fortification status. The estimated exposed population in drought-prone areas may not be the actual overview, as this study does not consider the regional-level adaptation mechanism to drought. Therefore, further studies on population exposure to drought should consider the regional fortification level. Furthermore, it has been recognized that GCM output-based projections typically insert some unavoidable uncertainties. Uncertainty could arise mainly due to model parameterization, internal variability, and GHG emission considerations. In addition, the PET calculation method, choice of drought indices, and population predictions are sources of uncertainty. In this study, we considered only hydrological drought to assess population exposure using the SPEI-12. Therefore, it is suggested to conduct a further study by considering other drought types under the latest CMIP6 scenarios.

This study has highlighted some key insights into initiating diverse policy interventions. In the near future, mitigation policy interventions for changing climates will be the pivotal basis to reduce drought-induced exposure in South Asian countries. Policymaking focusing on population growth control will be vital for mid- and long-term periods. These policy-interventions can be well-explained by the IPCC (2007) report that limiting global temperature rise to 1.5 °C compared to 2.0 °C can reduce the fraction of the global population exposure to climate-induced water stress by 50%. Reducing the cumulative Co_2 emissions is essential to limiting global warming. IPCC (2018) summarizes that to limit the warming of 1.5 °C under model scenarios, global anthropogenic net Co_2 emission is estimated to reduce by about 45% by 2030, and reach net-zero levels by 2045–2055. For holding global warming below 2.0 °C, anthropogenic Co_2 emissions are anticipated to decline 25% by the near-term period (around 2030), and net-zero level achieved by the long-term period (around 2065–2080). Therefore, the findings of this study emphasize on executing global emissions mitigation ambitions designed under the Paris Agreement. However, changes to the hotspots of population exposure in South Asia are identified, and the detailed findings provide guidance for drought monitoring and associated risk management. As the latest CMIP6 model output was used, the findings of this study can serves as a reasonable and reliable basis for significant implications on policy making in regard to water resource planning and migration management over South Asian countries.

Authors contributions

T. Jiang, and B.D. Su conceived the study. S.K. Mondal and J.L Huang contributed equally to this paper by performing analyses and drafting the paper. F. Thomas and Y.J. Wang calculated the SPEI-12 covering whole Asian area. G.J. Wang, and H. Tao integrated innovative ideas and improved the complete research and manuscript. Shanshan Wen and J.Q. Zhai performed downscaling and bias correction of the GCMs simulation and projection. All authors discussed the results and edited the manuscript.

Declaration of competing interest

The authors declare that they have no known competing financial interests or personal relationships that could have appeared to influence the work reported in this paper.

Acknowledgments

Our research work was jointly supported by the National Key Research and Development Program of China MOST (2018FY100501) and by the National Science Foundation of China (41671211 and 41661144027). The authors would like to thank the support given by the High-level Talent Recruitment Program of the Nanjing University of Information Science and Technology (NUIST) and the Guest Professor Program of the Xinjiang Institute of Ecology and Geography, CAS. All the authors express their gratitude to the World Climate Research Program's working group on coupled modelling for producing and publishing their GCM outputs publicly. We would like to acknowledge the availability of the national population data of South Asia for 1960–2016 (https://data.worldbank.org.cn/indicator/SP.POP.TOTL?end=2018&start=1960&view=chart). The population under five Shared Socioeconomic Pathways was freely obtained from Inter-Sectoral Impact Model Intercomparison Project (ISIMIP) and further re-gridded by the NUIST (https://geography.nuist.edu.cn/2019/1113/c1954a147560/page.htm). The gridded population of the world

(GPWv4) was freely obtained from the website (http://sedac.ciesin.columbia.edu/data/collection/gpw-v4/sets/browse). Authors are also thankful to the ISI-MIP for giving available observed datasets for bias correction.

Appendix A. Supplementary data

Supplementary data to this article can be found online at https://doi.org/10.1016/j.scitotenv.2021.145186.

References

Aadhar, S., Mishra, V., 2017. High-resolution near real-time drought monitoring in South Asia. Scientific Data 4 (1), 170145. https://doi.org/10.1038/sdata.2017.145.

Adnan, S., Ullah, K., Shuanglin, L., Gao, S., Khan, A.H., Mahmood, R., 2018. Comparisonof various drought indices to monitor drought status in Pakistan. Clim. Dyn. 51, 1885–1899. https://doi.org/10.1007/s00382-017-3987-0.

Ahmad, S., Hussain, Z., Qureshi, A.S., Majeed, R., Saleem, M., 2004. Drought Mitigation in Pakistan: Current Status and Options for Future Strategies. International Water Management Institute, Colombo, Sri Lanka.

Allen, R.G., Pereira, L.S., Raes, D., Smith, M., 1998. FAO Irrigation and Drainage Paper No. 56 - Crop Evapotranspiration. 56.

Almazroui, M., Saeed, S., Saeed, F., Islam, M.N., Ismail, M., 2020. Projections of precipitation and temperature over the south Asian countries in CMIP6. Earth Systems and Environment 4 (2), 297–320. https://doi.org/10.1007/s41748-020-00157-7.

Barnett, A.G., Tong, S., Clements, A.C.A., 2010. What measure of temperature is the best predictor of mortality? Environ. Res. 110 (6), 604–611. https://doi.org/10.1016/j.envres.2010.05.006.

Barthel, F., Neumayer, E., 2012. A trend analysis of normalized insured damage from natural disasters. Clim. Chang. 113 (2), 215–237. https://doi.org/10.1007/s10584-011-0331-2.

Cao, L., Fang, Yu., Jiang, T., et al., 2012. Advances in shared socioeconomic pathways for climate research and assessment. Climate Change Research 8 (1), 74–78 (in Chinese with English abstract).

Chen, H., Sun, J., 2015. Changes in drought characteristics over China using the standardized precipitation evapotranspiration index. J. Clim. 28 (13), 5430–5447. https://doi.org/10.1175/JCLI-D-14-00707.1.

Chen, J., Liu, Y., Pan, T., Liu, Y., Sun, F., Ge, Q., 2018. Population exposure to droughts in China under the 1.5 °C global warming target. Earth System Dynamics 9 (3), 1097–1106. https://doi.org/10.5194/esd-9-1097-2018.

Cook, B.I., Mankin, J.S., Anchukaitis, K.J., 2018. Climate change and drought: from past to future. Current Climate Change Reports 4 (2), 164–179. https://doi.org/10.1007/s40641-018-0093-2.

Dai, A., 2011. Characteristics and trends in various forms of the Palmer Drought Severity Index during 1900–2008. J. Geophys. Res. 116 (D12), 1248–1256.

Di Luca, A., Pitman, A.J., Elía, R., 2020. Decomposing temperature extremes errors in CMIP5 and CMIP6 models. Geophys. Res. Lett. 47 (14). https://doi.org/10.1029/2020GL088031.

Donohue, K., Rubio de Casas, R., Burghardt, L., Kovach, K., Willis, C.G., 2010. Germination, postgermination adaptation and species ecological ranges. Annu. Rev. Ecol. Evol. Syst. 41, 293–319. https://doi.org/10.1146/annurev-ecolsys-102209-144715.

Eyring, V., Bony, S., Meehl, G.A., Senior, C.A., Stevens, B., Stouffer, R.J., Taylor, K.E., 2016. Overview of the Coupled Model Intercomparison Project Phase 6 (CMIP6) experimental design and organization. Geosci. Model Dev. 9, 1937–1958. https://doi.org/10.5194/gmd-9-1937-2016.

Field, C.B., Barros, V., Stocker, T.F., Dahe, Q., Jon Dokken, D., Ebi, K.L., Field, C.B., Barros, V., Stocker, T.F., Dahe, Q., et al., 2012. Managing the risks of extreme events and disasters to advance climate change adaptation. Managing the Risks of Extreme Events and Disasters to Advance Climate Change Adaptation: Special Report of the Intergovernmental Panel on Climate Change. 9781107025. Cambridge University Press, Cambridge. https://doi.org/10.1017/CBO9781139177245.

Global Climate Risk Index, 2018. Who Suffers Most from ExtremeWeather Events? Weather-Related Loss Events in 2016 and 1997 to 2016. Germanwatch, Bonn/Berlin, Ger.

Guo, H., Bao, A., Liu, T., Jiapaer, G., Ndayisaba, F., Jiang, L., et al., 2018. Spatial and temporal characteristics of droughts in Central Asia during 1966–2015. Sci. Total Environ. 624, 1523–1538. https://doi.org/10.1016/j.scitotenv.2017.12.120.

Gupta, V., Jain, M.K., 2018. Investigation of multi-model spatiotemporal mesoscale drought projections over India under climate change scenario. J. Hydrol. 567 (October), 489–509. https://doi.org/10.1016/j.jhydrol.2018.10.012.

Ha, K., Moon, S., Timmermann, A., Kim, D., 2020. Future changes of summer monsoon characteristics and evaporative demand over Asia in CMIP6 simulations. Geophys. Res. Lett. 47 (8), 1–10. https://doi.org/10.1029/2020gl087492.

Huang, J., Wang, Y., Fischer, T., Su, B., Li, X., Jiang, T., 2017. Simulation and projection of climatic changes in the Indus River Basin, using the regional climate model COSMO-CLM. Int. J. Climatol. 37 (5), 2545–2562. https://doi.org/10.1002/joc.4864.

IPCC, 2007. Climate Change 2014: The Physical Science Basis. Cambridge University Press, Cambridge.

IPCC, 2012. Managing the risks of extreme events and disasters to advance climate change adaptation. A Special Report of Working Groups I and II of the Intergovernmental Panel on Climate Change. Cambridge University Press, Cambridge, UK, and New York, NY, USA.

IPCC, 2013. Climate change 2013: the physical science basis. In: Stocker, T.F., Qin, D., Plattner, M., Tibnor, S.K., Allwn, J., Boschung, A., Nauels, Y., Bex, V., Midgley, P.M. (Eds.), Working group I contribution to the fifth assessment report of the Intergovernmental Panel on Climate Change (IPCC). Cambridge University Press, Cambridge, United Kingdom and New York, NY, USA.

IPCC, 2018. In: Masson-Delmotte, V., Zhai, P., Pörtner, H.-O., Roberts, D., Skea, J., Shukla, P.R., Pirani, A., Moufouma-Okia, W., Péan, C., Pidcock, R., Connors, S., Matthews, J.B.R., Chen, Y., Zhou, X., Gomis, M.I., Lonnoy, E., Maycock, T., Tignor, M., Waterfeld, T. (Eds.), Global Warming of 1.5°C. An IPCC Special Report on the Impacts of Global Warming of 1.5°C Above Pre-Industrial Levels and Related Global Greenhouse Gas Emission Pathways, In the Context of Strengthening the Global Response to the Threat of Climate Change, Sustainable Development, and Efforts to Eradicate Poverty.

Irannezhad, M., Ahmadi, B., Kløve, B., Moradkhani, H., 2017. Atmospheric circulation patterns explaining climatological drought dynamics in the boreal environment of Finland, 1962–2011. Int. J. Climatol. 37, 801–817. https://doi.org/10.1002/joc.5039.

Jiang, J., Zhou, T., Chen, X., Zhang, L., 2020a. Future changes in precipitation over Central Asia based on CMIP6 projections. Environ. Res. Lett. https://doi.org/10.1088/1748-9326/ab7d03.

Jiang, T., Zhao, J., Jing, C., et al., 2017. National and provincial population projected to 2100 under shared socioeconomic pathways. J. Climate Change Research 13 (2), 128–137 (in Chinese with English abstract).

Jiang, T., Zhao, J., Jing, C., et al., 2018a. Projection of National and provincial economy under shared socioeconomic pathways. J. Climate Change Research 14 (1), 50–58 (in Chinese with English abstract).

Jiang, T., Wang, Y., Yuan, J., et al., 2018b. Projection of population and economy in the belt and road countries (2020–2060). J. Climate Change Research 14 (2), 155–164 (in Chinese with English abstract).

Jiang, T., Wang, Y., Su, B., Zhai, J., Tao, H., Jiang, C., Huang, J., Wen, S., PAN, J., 2020b. Perspectives of human activities in global climate change: evolution of Socio-economic scenarios. Journal of NUIST 12 (1), 68–80 (In Chinese).

Jing, C., Tao, H., Jiang, T., Wang, Y.J., Zhai, J.Q., Cao, L.G., Su, B.D., 2020. Population, urbanization and economic scenarios over the belt and road region under the shared socioeconomic pathways. J. Geogr. Sci. 30 (1), 68–84.

Jones, B., O'Neill, B.C., 2016. Spatially explicit global population scenarios consistent with the shared socioeconomic pathways. Environ. Res. Lett. 11, 084003. https://doi.org/10.1088/1748-9326/11/8/084003.

Jones, B., O'Neill, B.C., McDaniel, L., McGinnis, S., Mearns, L.O., Tebaldi, C., 2015. Future population exposure to US heat extremes. Nat. Clim. Chang. 5 (7), 652–655. https://doi.org/10.1038/nclimate2631.

Lehner, F., Coats, S., Stocker, T.F., Pendergrass, A.G., Sanderson, B.M., Raible, C.C., Smerdon, J.E., 2017. Projected drought risk in 1.5 °C and 2 °C warmer climates. Geophys. Res. Lett. 44 (14), 7419–7428. https://doi.org/10.1002/2017GL074117.

Liao, X., Xu, W., Zhang, J., Li, Y., Tian, Y., 2019. Global exposure to rainstorms and the contribution rates of climate change and population change. Sci. Total Environ. 663, 644–653. https://doi.org/10.1016/j.scitotenv.2019.01.290.

Lin, Q., Wang, Y., Glade, T., Zhang, J., Zhang, Y., 2020. Assessing the spatiotemporal impact of climate change on event rainfall characteristics influencing landslide occurrences based on multiple GCM projections in China. Clim. Chang. 162, 761–779. https://doi.org/10.1007/s10584-020-02750-1.

McKenna, S., Santoso, A., Gupta, A.S., Taschetto, A.S., Cai, W., 2020. Indian Ocean dipole in CMIP5 and CMIP6: characteristics, biases, and links to ENSO. Sci. Rep. 10.

Miao, L., Li, S., Zhang, F., Chen, T., Shan, Y., Zhang, Y., 2020. Future drought in the dry lands of Asia under the 1.5 and 2.0 °C warming scenarios. Earth's Future 8 (6). https://doi.org/10.1029/2019EF001337.

Mishra, A.K., Singh, V.P., 2010. A review of drought concepts. J. Hydrol. 391 (1–2), 202–216. https://doi.org/10.1016/j.jhydrol.2010.07.012.

Mishra, V., Aadhar, S., Asoka, A., Pai, S., Kumar, R., 2016. On the frequency of the 2015 monsoon season drought in the Indo-Gangetic Plain. Geophys. Res. Lett. 43 (23), 12,102–12,112. https://doi.org/10.1002/2016GL071407.

Nath, R., Cui, X., Nath, D., Graf, H.F., Chen, W., Wang, L., et al., 2017. CMIP5 multimodel projections of extreme weather events in the humid subtropical Gangetic Plain region of India. Earth's Future 5 (2), 224–239. https://doi.org/10.1002/2016EF000482.

O'Neill, B.C., Tebaldi, C., Van Vuuren, D.P., Eyring, V., Friedlingstein, P., Hurtt, G., et al., 2016. The Scenario Model Intercomparison Project (ScenarioMIP) for CMIP6. Geosci. Model Dev. 9 (9), 3461–3482. https://doi.org/10.5194/gmd-9-3461-2016.

O'Neill, B.C., Kriegler, E., Ebi, K.L., Kemp-Benedict, E., Riahi, K., Rothman, D.S., et al., 2017. The roads ahead: narratives for shared socioeconomic pathways describing world futures in the 21st century. Glob. Environ. Chang. 42, 169–180. https://doi.org/10.1016/j.gloenvcha.2015.01.004.

Pierce, D.W., Barnett, T.P., Santer, B.D., Gleckler, P.J., 2009. Selecting global climate models for regional climate change studies. Proc. Natl. Acad. Sci. U. S. A. 106 (21), 8441–8446. https://doi.org/10.1073/pnas.0900094106.

Schleussner, C., Deryng, D., D'haen, S., Hare, W., Lissner, T., Ly, M., et al., 2018. 1.5°C hotspots: climate hazards, vulnerabilities, and impacts. Annu. Rev. Environ. Resour. 43 (1), 135–163. https://doi.org/10.1146/annurev-environ-102017-025835.

van der Schrier, G., Jones, P.D., Briffa, K.R., 2011. The sensitivity of the PDSI to the Thornthwaite and penman-Monteith parameterizations for potential evapotranspiration. J. Geophys. Res. 116 (D3), D03106. https://doi.org/10.1029/2010JD015001.

Sheffield, J., Wood, E.F., Roderick, M.L., 2012. Little change in global drought over the past 60 years. Nature 491 (7424), 435–438. https://doi.org/10.1038/nature11575.

Shrestha, A., Rahaman, M.M., Kalra, A., Jogineedi, R., Maheshwari, P., 2020. Climatological drought forecasting using bias corrected CMIP6 climate data: a case study for India. Forecasting 2, 59–84. https://doi.org/10.3390/forecast2020004.

Smirnov, O., Zhang, M., Xiao, T., Orbell, J., Lobben, A., Gordon, J., 2016. The relative importance of climate change and population growth for exposure to future

extreme droughts. Clim. Chang. 138 (1–2), 41–53. https://doi.org/10.1007/s10584-016-1716-z.
Su, B., Huang, J., Gemmer, M., Jian, D., Tao, H., Jiang, T., Zhao, C., 2016. Statistical downscaling of CMIP5 multi-model ensemble for projected changes of climate in the Indus River Basin. Atmos. Res. 178–179, 138–149. https://doi.org/10.1016/j.atmosres.2016.03.023.
Su, B., Huang, J., Fischer, T., Wang, Y., Kundzewicz, Z.W., Zhai, J., et al., 2018. Drought losses in China might double between the 1.5 °C and 2.0 °C warming. Proc. Natl. Acad. Sci., 201802129 https://doi.org/10.1073/pnas.1802129115.
Su, B., Huang, J., Mondal, S.K., Zhai, J., Wang, Y., Wen, S., Gao, M., Lv, Y., Jiang, S., Jiang, T., Li, A., 2020. Insight from CMIP6 SSP-RCP scenarios for future drought characteristics in China. Atmos. Res. 105375. https://doi.org/10.1016/j.atmosres.2020.105375.
Sun, H., Wang, Y., Chen, J., Zhai, J., Jing, C., Zeng, X., et al., 2017. Exposure of population to droughts in the Haihe River basin under global warming of 1.5 and 2.0 °C scenarios. Quat. Int. 453, 74–84. https://doi.org/10.1016/j.quaint.2017.05.005.
Tan, C., Yang, J., Li, M., 2015. Temporal-spatial variation of drought indicated by SPI and SPEI in Ningxia Hui Autonomous Region, China. Atmosphere (Basel). 6, 1399–1421. https://doi.org/10.3390/atmos6101399.
Tokarska, K.B., Stolpe, M.B., Sippel, S., Fischer, E.M., Smith, C.J., Lehner, F., Knutti, R., 2020. Past warming trend constrains future warming in CMIP6 models. Sci. Adv. doi https://doi.org/10.1126/sciadv.aaz9549.
Trenberth, K.E., Dai, A., Van Der Schrier, G., Jones, P.D., Barichivich, J., Briffa, K.R., Sheffield, J., 2013. Global warming and changes in drought. Nat. Clim. Chang. 4, 17–22. https://doi.org/10.1038/nclimate2067.
Trenberth, K.E., Dai, A., van der Schrier, G., Jones, P.D., Barichivich, J., Briffa, K.R., Sheffield, J., 2014. Global warming and changes in drought. Nat. Clim. Chang. 4 (1), 17–22. https://doi.org/10.1038/nclimate2067.
Trenberth, K.E., Fasullo, J.T., Shepherd, T.G., 2015. Attribution of climate extreme events. Nat. Clim. Chang. 5, 725–730. https://doi.org/10.1038/nclimate2657.
United Nations, 2017a. Department of Economic and Social Affairs, population division. World Population Prospects: The 2017 Revision, Key Findings and Advance Tables. ESA/P/WP/248. United Nations, New York.
United Nations (2017b) Department of Economic and Social Affairs, population division, 2017. World Population Prospects: The 2017 Revision, Volume II: Demographic Profiles. ST/ESA/SER.A/400. United Nations, New York.
United Nations, 2018. Department of Economic and Social Affairs, population division. World Urbanization Prospects: The 2018 Revision, Methodology. Working paper no. ESA/P/WP. United Nations, New York, p. 252.
United Nations International Strategy for Disaster Reduction (UNISDR), 2009. Drought risk reduction framework and practices: Contributing to the implementation of the Hygo framework for action. United Nations Secretariat of the International Strategy for Disaster 5 Reduction (UNISDR). Swizerland, Geneva.
United Nations International Strategy for Disaster Reduction (UNISDR), 2017. Terminology. https://www.unisdr.org/we/inform/terminology#letter-e/.
Vicente-Serrano, S.M., Beguería, S., López-Moreno, J.I., 2010. A multiscalar drought index sensitive to global warming: the standardized precipitation evapotranspiration index. J. Clim. 23, 1696–1718. https://doi.org/10.1175/2009JCLI2909.1.
Vicente-Serrano, S.M., Zouber, A., Lasanta, T., Pueyo, Y., 2012. Dryness is accelerating degradation of vulnerable shrublands in semiarid Mediterranean environments. Ecol. Monogr. 82 (4), 407–428.
Vicente-Serrano, S.M., Van der Schrier, G., Beguería, S., Azorin-Molina, C., Lopez-Moreno, J.I., 2015. Contribution of precipitation and reference evapotranspiration to drought indices under different climates. J. Hydrol. 526, 42–54. https://doi.org/10.1016/j.jhydrol.2014.11.025.
Wang, A., Wang, Y., Su, B., Kundzewicz, Z.W., Tao, H., Wen, S., et al., 2020. Comparison of changing population exposure to droughts in river basins of the Tarim and the Indus. Earth's Future, 0–1 https://doi.org/10.1029/2019ef001448.
Wang, Y., Jing, C., Cao, L., et al., 2017. Projection of population and economy in the belt and road countries (2020–2060). J. Climate Change Research 13 (4), 327–336 (in Chinese with English abstract).
Watterson, I.G., Bathols, J., Heady, C., 2014. What influences the skill of climate models over the continents? Bull. Am. Meteorol. Soc. 95, 689–700.
Watts, N., Adger, W.N., Agnolucci, P., Blackstock, J., Byass, P., Cai, W., et al., 2015. Health and climate change: policy responses to protect public health. Lancet 386 (10006), 1861–1914. https://doi.org/10.1016/S0140-6736(15)60854-6.
Wen, S., Wang, A., Tao, H., Malik, K., Huang, J., Zhai, J., et al., 2019. Population exposed to drought under the 1.5 °C and 2.0 °C warming in the Indus River Basin. Atmos. Res. 218 (December 2018), 296–305. https://doi.org/10.1016/j.atmosres.2018.12.003.
Wilhite, D.A., Sivakumar, M.V.K., Pulwarty, R., 2014. Managing drought risk in a changing climate: the role of national drought policy. Weather and Climate Extremes 3, 4–13. https://doi.org/10.1016/j.wace.2014.01.002.
WMO, 2013. The Global Climate 2001–2010: a Decade of Climate Extremes. World Meteorological Organization.
World Bank, 2016. South Asia Economic Updates 2010: Moving Up, Looking East. World Bank, Washington DC, USA.
Xin, X., Wu, T., Zhang, J., Yao, J., Fang, Y., 2020. Comparison of CMIP6 and CMIP5 simulations of precipitation in China and the east Asian summer monsoon. Int. J. Climatol. 40, 6423–6440.
Yevjevich, V.M., 1969. An objective approach to definitions and investigations of continental hydrologic droughts. J. Hydrol. 7 (3), 353. https://doi.org/10.1016/0022-1694.
Zhai, J., Mondal, S.K., Fischer, T., Wang, Y., Su, B., Huang, J., et al., 2020. Future drought characteristics through a multi-model ensemble from CMIP6 over South Asia. Atmos. Res. 246, 105111. https://doi.org/10.1016/j.atmosres.2020.105111.
Zhang, W., Li, Y., Li, Z., Wei, X., Ren, T., Liu, J., Zhu, Y., 2020. Impacts of climate change, population growth, and urbanization on future population exposure to long-term temperature change during the warm season in China. Environ. Sci. Pollut. Res. 27, 8481–8491. https://doi.org/10.1007/s11356-019-07238-9.
Zhou, J., Wang, Y.J., Su, B.D., Wang, A.Q., Tao, H., Zhai, J.Q., Kundzewicz, Z.W., Jiang, T., 2020. Choice of potential evapotranspiration formulas influences drought assessment: a case study in China. Atmos. Res. https://doi.org/10.1016/j.atmosres.2020.104979.